Published November 25, 2013

RNA recognition by human TLR8 can lead to autoimmune inflammation

Cristiana Guiducci,[1] Mei Gong,[1] Alma-Martina Cepika,[2] Zhaohui Xu,[2] Claudio Tripodo,[3] Lynda Bennett,[2] Chad Crain,[1] Pierre Quartier,[4] John J. Cush,[2] Virginia Pascual,[2,5] Robert L. Coffman,[1] and Franck J. Barrat[1]

[1]Dynavax Technologies Corporation, Berkeley, CA 94710
[2]Baylor Institute for Immunology Research, Dallas, TX 75204
[3]Department of Human Pathology, Tumor Immunology Section, University of Palermo School of Medicine, 90128 Palermo, Italy
[4]Hematology-Immunology-Rheumatology Unit, AP-HP, Necker Enfants Malades Hospital, 75015 Paris, France
[5]Texas Scottish Rite Hospital, Dallas, TX 75219

Studies on the role of the RNA receptor TLR8 in inflammation have been limited by its different function in human versus rodents. We have generated multiple lines of transgenic mice expressing different levels of human TLR8. The high copy number chimeras were unable to pass germline; developed severe inflammation targeting the pancreas, salivary glands, and joints; and the severity of the specific phenotypes closely correlated with the huTLR8 expression levels. Mice with relatively low expression levels survived and bred successfully but had increased susceptibility to collagen-induced arthritis, and the levels of huTLR8 correlated with proinflammatory cytokines in the joints of the animals. At the cellular level, huTLR8 signaling exerted a DC-intrinsic effect leading to up-regulation of co-stimulatory molecules and subsequent T cell activation. A pathogenic role for TLR8 in human diseases was suggested by its increased expression in patients with systemic arthritis and the correlation of TLR8 expression with the elevation of IL-1β levels and disease status. We found that the consequence of self-recognition via TLR8 results in a constellation of diseases, strikingly distinct from those related to TLR7 signaling, and points to specific inflammatory diseases that may benefit from inhibition of TLR8 in humans.

CORRESPONDENCE
Cristiana Guiducci:
cguiducci@dynavax.com

Abbreviations used: BAC, bacterial artificial chromosome; ES, embryonic stem; mDC, myeloid DC; PDC, plasmacytoid DC; RNP, ribonucleoprotein; SoJIA, systemic onset juvenile idiopathic arthritis; ssRNA, single-stranded RNA.

Activation of the innate response initiated by TLRs is an essential mechanism of defense against many pathogens; however, TLR can also respond to endogenous ligands, potentially leading to autoimmunity if not properly controlled. This is particularly clear for the nucleic acid receptors TLR7 and 9, which appear to mediate the pathogenesis of several autoimmune diseases, most notably lupus. In lupus, TLR7 and TLR9 recognition of endogenous RNA and DNA, respectively, results in the production of type I IFNs and the anti-DNA and ribonucleoprotein (RNP) autoantibodies characteristic of the disease. In mice, an increased copy number of the TLR7 gene leads to a lupus-like syndrome characterized by accumulation of RNP-specific autoantibodies (Pisitkun et al., 2006; Subramanian et al., 2006; Deane et al., 2007; Walsh et al., 2012). In lupus-prone MRL/lpr mice, deletion of the TLR7 gene reduced the level of anti-RNP autoantibodies but not the level of anti-dsDNA antibodies, which depends on TLR9 expression (Christensen et al., 2006; Nickerson et al., 2010). These results clearly suggest that the two major classes of autoantigens targeted in lupus, DNA- and RNA-binding proteins are specifically controlled by TLR9 and TLR7, respectively. Furthermore, treatment of the lupus prone (NZBxNZW)F1 mice with a TLR7 and 9 inhibitor leads to reduced symptoms and increased survival (Barrat et al., 2007). It is not known whether the second endosomal receptor for single-stranded RNA (ssRNA), TLR8, could likewise

F.J. Barrat's present address is Hospital for Special Surgery, New York, NY 10021.

The Rockefeller University Press $30.00
J. Exp. Med. 2013
www.jem.org/cgi/doi/10.1084/jem.20131044

Published November 25, 2013

mediate autoimmunity and, if so, which diseases would result from its dysfunction.

In humans, TLR8, like TLR7, recognizes viral RNA, self-RNA within snRNP autoantibodies complexes, and several classes of small molecule agonists (Gorden et al., 2005; Vollmer et al., 2005; Forsbach et al., 2008; Gantier et al., 2008; Ablasser et al., 2009; Liu et al., 2010). However, numerous differences exist among these two receptors. TLR8 is preferentially activated by ssRNA rich in AU, whereas sequences rich in GU preferentially activate TLR7 (Forsbach et al., 2008). Additionally, TLR8 senses ssRNA through its ability to form secondary structures, a characteristic not required for TLR7 activation (Sarvestani et al., 2012). Lastly, the pattern of expression of the two receptors differs among human blood cells. TLR7 is largely coexpressed with TLR9, primarily on B cells and PDCs (plasmacytoid DCs), whereas TLR8 is absent in these cells and abundantly expressed in monocytes, myeloid DCs (mDCs), and neutrophils (see Fig. 9 A; Hattermann et al., 2007; Forsbach et al., 2008; Janke et al., 2009), suggesting that activation of human TLR8 by endogenous ligands might lead to a different spectrum of inflammatory disease than the one resulting from activation of TLR7 and TLR9.

Circumstantial evidence implicates a role of TLR8 in human diseases, including RA (Sacre et al., 2008), antiphospholipid syndrome (APS; Döring et al., 2010), and IBD (Prinz et al., 2011). These reports rely mostly on gene polymorphism and correlative studies. The absence of small animal models has limited studies of the disease associations of TLR8 signaling. Mouse TLR8 does not recognize ssRNA ligands, RNA viruses, or small molecules that are potent agonists for human TLR8 (Hemmi et al., 2002; Heil et al., 2004) a difference caused by the absence of 5 aa that are necessary for RNA recognition by human TLR8 (Liu et al., 2010). Thus, the role of self-recognition by TLR8 cannot be meaningfully studied in current mouse models of autoimmunity and a more relevant small animal model would represent a significant advantage in the field. In this study, we have thus generated multiple human TLR8 transgenic lines of ES cells and generated chimeric mice from these ES lines to study human TLR8 function in vivo.

RESULTS

Mice with high expression of human TLR8 develop multiorgan inflammatory syndrome

To develop a small animal model to study human TLR8 function, we generated transgenic mice expressing human TLR8 under the control of human TLR8 genomic regulatory regions. A BAC clone containing the complete human TLR7 and TLR8 genomic region was modified to delete the huTLR7 coding region, leaving only the huTLR8 gene capable of expression. Transfection of a C57BL/6 ES cell line with this construct produced many clones, four of which were selected to generate transgenic mice (Fig. S1). Chimeras produced from three of these clones (6, 12, and 23) developed a wasting disease, surviving from 23 and 140 d (Fig. 1 A), and failing to breed successfully. The level of huTLR8 mRNA expression in these chimeras correlated negatively with survival (Fig. 1 B). Interestingly, spontaneous disease was observed even in mice with as few as 20% of the blood cells derived from the huTLR8 transgenic ES cells, demonstrating a strong dominant biological effect (Fig. 1 C). Chimeras from a fourth ES clone, Clone 8, (TLR8TgCL8) had a lower level of transgene expression (Fig. 1 D), and bred normally, allowing establishment of a stable transgenic line on C57BL/6 background.

PBMCs isolated from all the transgenic lines responded to the RNA-based ligand of human TLR8 (ORN-8L; Lan et al., 2007; Fig. 1 E), whereas PBMCs from nontransgenic mice were unresponsive to these ligands (Fig. 1 E). These data demonstrated that huTLR8 is active when expressed in mice and that is not constitutively activated in the transgenic chimeras, as no spontaneous production of cytokines was detected in cultured PBMCs in the absence of TLR8 agonists (Fig. 1 E). Proteolysis by endolysosomal protease is required for signaling of TLR7, TLR9, and TLR3 (Ewald et al., 2011; Maschalidi et al., 2012). Treatment with bafilomycin A1, an inhibitor of the vacuolar ATPase which blocks acid-dependent protease activity, prevents TLR8 activation both in human PBMCs and PBMCs from huTLR8 transgenic mice (Fig. 1, F and G). These data demonstrate that the dependence on receptor proteolysis is preserved when human TLR8 is expressed in mouse cells.

Histopathological evaluation of the chimeras revealed inflammation in the pancreas, kidneys, liver, salivary glands, and the joints. The disease patterns in mice generated from the three independent ES clones were essentially the same, suggesting that the phenotype is due to the transgene itself, not to an insertional mutation in the host genome (Fig. 2, A and B; and Fig. S2 A). The pancreas was the most severely affected organ and the likely cause of death in these mice, with pancreatic acinar tissue substantially effaced by inflammatory cells, primarily macrophages, lymphocytes, and neutrophils. Residual islets could be identified within the inflammatory tissue, suggesting that the exocrine pancreas was the main target of the inflammatory reaction (Fig. 2 A, I and II; and Fig. S2, A and B). Kidney sections revealed two prominent types of lesions: pyelitis (Fig. 2 A, III and IV) and glomerulonephritis (Fig. 2 A, V and VI). Liver hepatic sections (Fig. 2 A, VII and VIII) revealed an inflammatory reaction mainly localized in the portal triads (Fig. S2 A). The inflammatory changes associated with the bile ducts are consistent with an autoimmune origin resembling autoimmune cholangiopathy in humans. Similarly affected were salivary glands that were severely compromised by an inflammatory infiltrate similar to that seen in the other organs (not depicted).

Lungs, brain, heart, and stomach tissues were not affected, suggesting selective inflammation of specific tissues. Serum levels of several inflammatory cytokines were elevated in huTLR8Tg chimeras (Fig. 2 C) and corresponding elevation of the mRNA of these cytokines were measured in pancreas of the affected animals (Fig. 2 D). Increased levels of antinuclear antibodies, dsDNA antibodies, and

Published November 25, 2013

anti-RNPs (Fig. 2 E) were also measured at sacrifice in moribund chimeric mice.

DC-intrinsic huTLR8 activation and subsequent T cell activation promote the inflammatory syndrome

This characteristic pattern of spontaneous multiorgan inflammation could reflect either responses intrinsic to the inflammatory cells themselves or the consequences of transgene expression in cells of the affected tissues, or both. To test these alternatives, bone marrow from each of the three independent huTLR8-expressing chimeras was transferred to irradiated congenic B6SJL mice. All reconstituted mice spontaneously developed a disease pattern remarkably similar to that observed in the chimeras, demonstrating that the expression of huTLR8 in the hematopoietic compartment is sufficient to generate the full spectrum of inflammatory disease (Fig. 3 A). Similar to what is observed in the chimeras (Fig. 1 B), huTLR8 gene expression level in the BM-transplanted animals correlated negatively with survival (Fig. S2 C). No difference was found in either the number or activation state of T cells in the BM of huTLR8Tg chimeras, compared with BM from WT mice, suggesting that disease in reconstituted mice did not result simply from the transfer of effector T cells (unpublished data). Organs of the reconstituted mice showed a pattern of severe inflammation in pancreas, liver, and salivary glands comparable to that in chimeric huTLR8Tg mice, and pancreas failure was similarly considered the primary cause of death (Fig. 3 B). However, huTLR8Tg reconstituted mice, in contrast to transgenic chimeras, showed no evidence for glomerulonephritis or kidney pyelitis (Fig. 3 B), and circulating antibodies against self-nucleic acids were not detected (not depicted). This could be due to the more rapid response observed in the reconstituted mice, but this also suggests that anti-nucleic acid autoantibodies contribute to the glomerulonephritis in huTLR8Tg chimeras but are not required for inflammation in the other affected organs.

Unlike chimeras, virtually all BM-derived cells were of transgenic origin, simplifying the analysis of the expression patterns of huTLR8 in the hematopoietic compartment. The distribution of huTLR8 among mouse blood cells was similar to its expression pattern in human leukocyte subsets, suggesting that the disease in mice was not due to a highly atypical pattern of cellular expression (Fig. 3 C).

To better understand the pathogenic changes, we analyzed the cellular compartment in the chimeric mice. The absolute number of circulating leukocytes in the blood and in the spleens was significantly decreased in huTLR8Tg chimeras (Fig. 4 A). The observed leukopenia is the result of a decreased

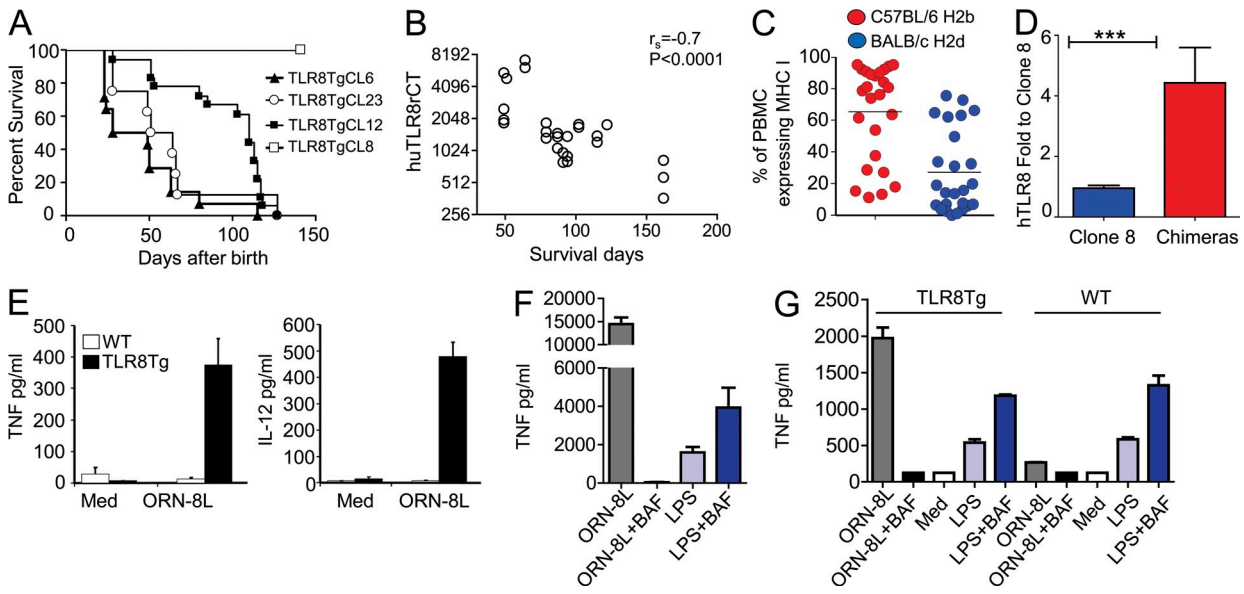

Figure 1. huTLR8 expression level strictly correlate with decrease survival in chimeric mice. (A) Mice were generated with a varying number of copies of huTLR8. Mice were from clone 6 (CL; $n = 14$), clone 23 ($n = 8$), clone 12 ($n = 44$), and clone 8 ($n = 18$). (B) Data from spleens was collected from moribund animals and TaqMan was used to evaluate huTLR8 expression. huTLR8 expression was plotted against survival time. 26 spleens ($n = 22$ from clone 12; $n = 4$ from clone 23) are shown. (C) PBMCs from huTLR8Tg chimeras were assessed by flow cytometry for expression of H2b (C57BL/6; expressing the transgene) or H2d haplotypes (BALB WT). From 25 mice ($n = 21$ from clone 12; $n = 3$ from clone 23; $n = 1$ from clone 6). (D) Human TLR8 expression level in blood from huTLR8Tg chimeras (total number of mice 26; $n = 21$ from clone 12; $n = 3$ from clone 23; $n = 2$ from clone 6) and from TLR8TgCL8 ($n = 36$) was evaluated by TAQMAN. Data are expressed as fold compared with huTLR8 expression level in clone 8 (E). 5×10^5 PBMCs from huTLR8Tg chimeras or C57BL/6 WT animals were stimulated with a specific RNA-based TLR8 agonist, ORN-8L, and 24 h later supernatants were harvested and assayed for TNF levels by ELISA; data are cumulative of $n = 4$ mice (mean ± SEM), 2 mice from TLR8TgCL12, 1 mice from TLR8TgCL6 and 1 mice from TLR8TgCL23. Data are from a representative experiment out of three independent experiments. (F and G) 5×10^5 PBMCs from human healthy donors (F; $n = 3$ donors; mean ± SEM), from TLR8TgCL12 chimeras, or from WT mice were stimulated with ORN-8L or LPS with or without bafilomycin A1 for 18 h. Stimulation with TLR4 ligand LPS was used as control (G; $n = 4$ mice; mean ± SEM).

Published November 25, 2013

number of lymphocytes both in circulation (Fig. 4 B) and in spleens (Fig. 4 A and Table 1).

We observed a slight increase in the percentage of circulating and splenic neutrophils and monocytes (Table 1), which is likely due to the decrease in lymphocyte number. Indeed, no significant increase in their absolute number was seen in the mice (Fig. 4 B). In chimeras, transgenic C57BL/6 and nontransgenic BALB/c cells could be distinguished by MHC haplotype, permitting comparison of the activation state of nontransgenic and huTLR8-expressing transgenic myeloid cells in the same animals. Enhanced expression of co-stimulatory molecules was observed only on the huTLR8 transgenic C57BL/6-DCs and monocytes, in both spleen and blood, showing that activation occurs only in the myeloid cells carrying the huTLR8 transgene and does not result from the elevated levels of inflammatory cytokines in these mice (Fig. 4 C). Similarly DCs and monocytes in WT mice transplanted with huTLR8Tg chimeras bone marrow were highly activated (Fig. 4 D) and this activation resulted in the increased ability of huTLR8Tg DCs to activate OT-II CD4 cells as compared with WT DCs (Fig. 4 E).

huTLR8Tg chimeras had a significant decrease of naive CD4 and CD8 T cells ($CD62L^{hi}$ $CD44^{low}$), paralleled by an increase of cells that were $CD44^{high}CD62L^{low}$, consistent with an effector/memory phenotype (Table 1). When stimulated with PMA/ionomycin in vitro, splenic CD4 and CD8 T cells

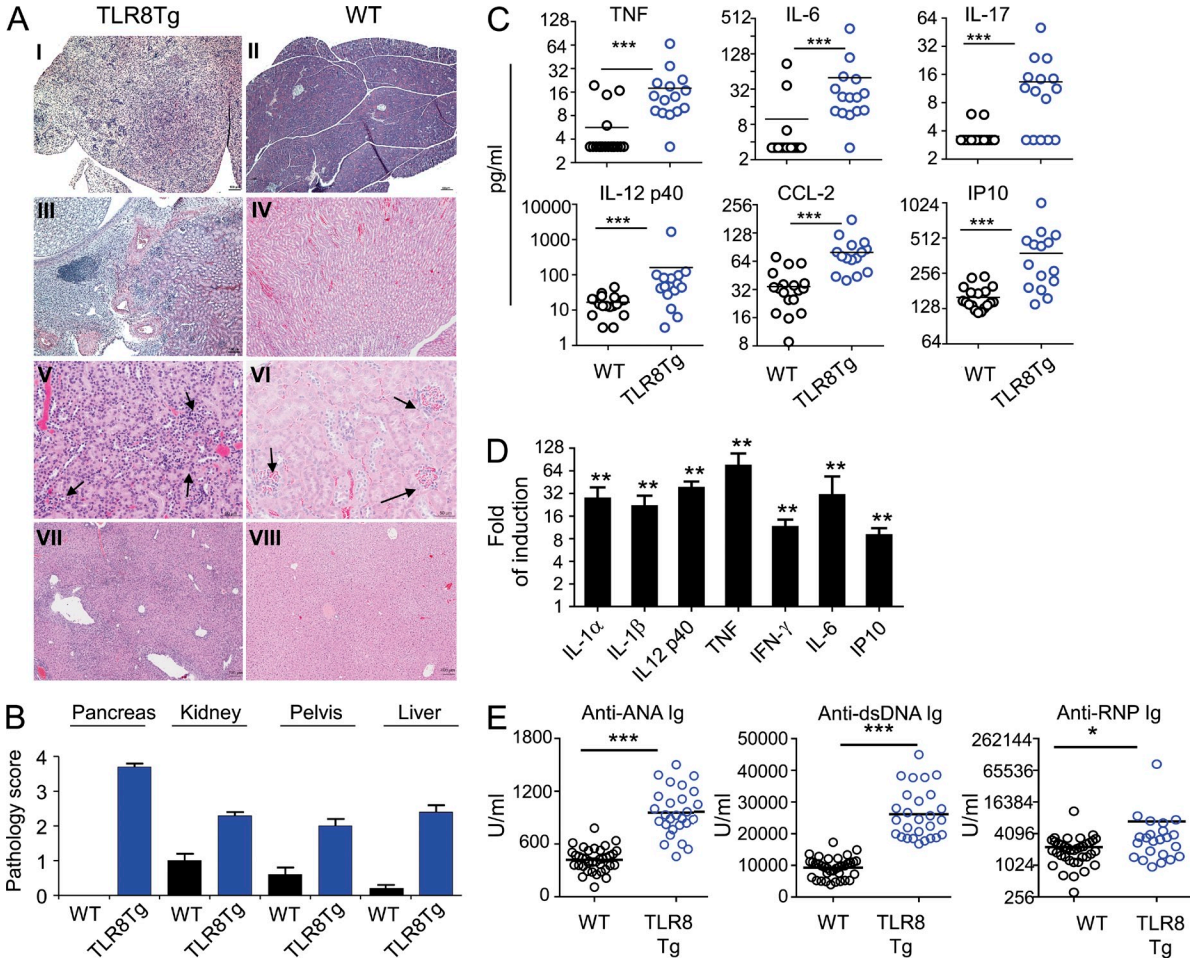

Figure 2. Multiorgan inflammation in huTLR8 chimera mice. (A) Organs from WT (II, IV, VI, VIII) or chimeric huTLR8Tg (I, III, V, VII) were stained with hematoxylin and eosin. Pancreas (I, II), kidney pelvis (III and IV), kidney (V and VI), and liver (VII and VIII). Arrows indicates normal glomerular structure in kidney sections from WT animals (VI) and evident glomerular abnormalities in kidney from huTLR8Tg animals (V). Sections of liver are represented in panel VII (huTLR8Tg) and panel VIII (WT). Additional pathology details in Fig. S2. Scale bar is 100 µm for all panels except V and VI which is 50 µm. (B) Cumulative data of the pathological score in the affected organs. $n = 28$ ($n = 18$ from clone 12; $n = 4$ from clone 23 and $n = 6$ from clone 6) and 14 for WT C57BL/6; (mean ± SEM). (C) Cytokines concentration in sera from TLR8TgCL12 ($n = 15$) and CTRL WT C57BL/6 mice ($n = 18$) was measured by Milliplex assay. (D) Pancreases from TLR8TgCL12 or CTRL WT C57BL/6 mice (total number of mice = 6/group) were harvested 40–60 d after birth, and the levels of pro-inflammatory genes were evaluated by TaqMan. Data are expressed as fold increase compared with CTRL mice (mean ± SEM). (E) huTLR8Tg animals were sacrificed when moribund (age ranged from 44 to 140 d). The titers of double-stranded DNA specific antibody (anti-ds DNA) and ribonucleoprotein (anti-RNP) specific antibody in the serum of TLR8TgCL12 chimeras ($n = 27$) and of age matched WT animals C57BL/6 ($n = 37$) were determined. *, $P \geq 0.05$; **, $P \geq 0.01$; ***, $P \geq 0.001$.

Published November 25, 2013

from huTLR8Tg chimera produced significantly more IFN-γ and TNF than cells from WT animals (Fig. 5, A and B), suggesting enrichment of Th1 cells.

T cells in huTLR8Tg mice do not express huTLR8, thus changes in T cell populations likely reflect interactions with huTLR8-expressing DCs. To address this hypothesis we looked in chimeras mice harboring T cells from both C57BL/6 and BALB/c haplotype and found that there was a clear preferential activation of the H2b$^+$ C57BL/6 T cells (Fig. 5, C–E).

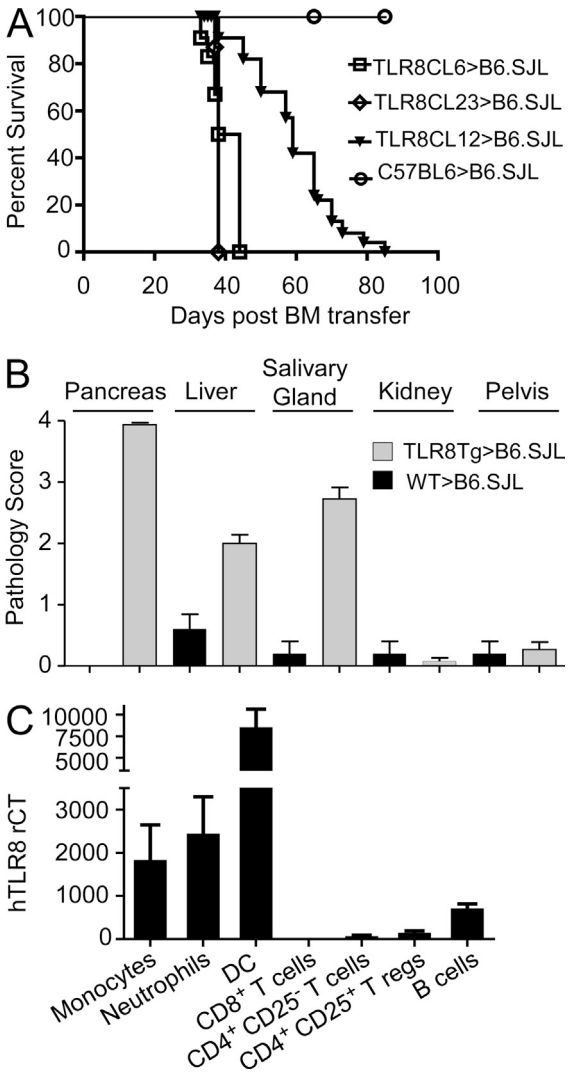

Figure 3. Pathology induced by huTLR8 expression is due to its activation in the hematopoietic compartment. (A) B6.SJLmice were transplanted with bone marrow from huTLR8Tg chimeras and monitored for survival. n = 45 for TLR8TgCL12>B6.SJL; n = 12 for TLR8TgCL6>B6.SJL; n = 12 for TLR8TgCL23>B6.SJL; and n = 12 for C57BL/6>B6.SJL. Data are cumulative of two independent experiments. (B) Organs from mice in A were harvested when mice were moribund. TLR8TgCL12>B6.SJL n = 19; n = 3 for TLR8TgCL6>B6.SJL; n = 3 for TLR8TgCL23>B6.SJL; and n = 9 for C57BL/6>B6.SJL (mean ± SEM). (C) Cellular subsets were isolated from spleens of B6.SJLmice transplanted with bone marrow from TLR8TgCL12 chimeras. Gene expression of huTLR8 was evaluated by TaqMan. Cumulative data from three independent experiments; n = 5–10. Mean ± SEM.

Human TLR8 signals independently of mouse TLR7

Previous findings have suggested cross-regulatory interactions between TLR7 and TLR8 in both expression and function (Wang et al., 2006; Demaria et al., 2010; Fukui et al., 2011). We found that the response to TLR8 ligands of TLR8TgCL8 backcrossed onto TLR7-deficient mice was not diminished, demonstrating that human TLR8 signals independently of mouse TLR7 (Fig. 6 A). In addition we found that the level of expression of mouse TLR7 mRNA in spleens and purified cellular subsets of chimeras huTLR8Tg mice was significantly decreased (Fig. 6, B and C) which is consistent with previous findings that, TLR7 expression is substantially increased in the absence of mouse TLR8 (Demaria et al., 2010).

Human TLR8 activation in the joints promotes spontaneous and induced arthritis in mice

The TLR8TgCL12 chimeras, which have the longest lifespan of the high huTLR8-expressing chimeras (Fig. 1 A), spontaneously developed arthritis in both forelimbs and hindlimbs in animals that survived at least 90 d (Fig. 7, A and B). The joints of these animals show typical features of arthritis, including synovial and periarticular inflammation, synovial hyperplasia, and cartilage damage (Fig. 7, A and B). This spontaneous arthritis is dependent on huTLR8; however, these animals usually die of pancreatitis soon after the onset of joint inflammation, limiting their utility for mechanistic studies. The stable transgenic mouse strain with relatively low expression of huTLR8, TLR8TgCL8, did not develop spontaneous arthritis, but did have enhanced susceptibility in the collagen-induced arthritis model (CIA; Fig. 8 A). The onset and the initial development of disease was comparable in TLR8TgCL8 and WT littermate controls; however, disease progression ceased at ∼4 wk in WT mice, typical of the mild disease seen in C57BL/6 mice. In contrast, disease progression continued in TLR8TgCL8 mice, leading ultimately to significant exacerbation of both clinical (Fig. 8 A) and pathological disease scores (Fig. 8, B–D). Whole ankle joints in TLR8TgCL8 mice showed increased synovial inflammation, pannus formation, cartilage destruction, and bone damage compared with WT controls (Fig. 8 E). In transgenic animals, the expression of huTLR8 in the joints correlated with the clinical score (unpublished data), as well as with the presence of macrophages (F4/80), and levels of proinflammatory cytokines such as TNF, IL1-β, IL-6, and IP-10 and of the metalloproteinases MMP-9 and MMP-3 (Fig. 8 F and not depicted). These findings demonstrate that although huTLR8 is not required for the onset of arthritis in this mouse model, signaling through TLR8 leads to progression and exacerbation of the relatively mild, self-limiting disease that develops in C57BL/6 mice strain.

Published November 25, 2013

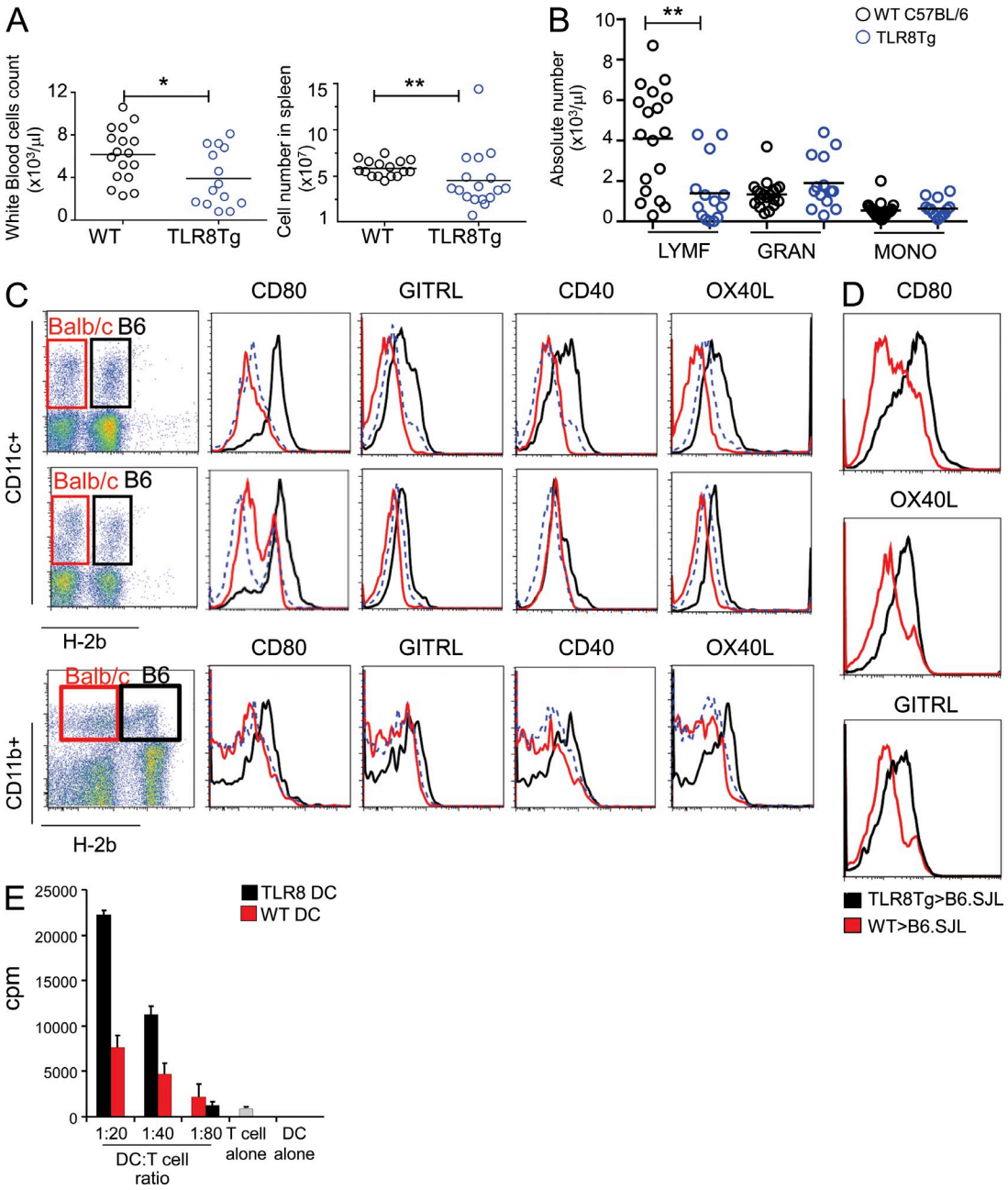

Figure 4. High expression level of huTLR8 leads to the intrinsic activation of DCs in mice. (A) Peripheral blood and spleens were harvested from high expressing huTLR8Tg chimeras (n = 14–17) or age-matched C57BL/6 (n = 17) mice, and cell numbers were assessed. (B) Absolute white cell numbers in blood of chimera mice from TLR8TgCL12 (n = 14) and WT C57BL/6 (n = 18). A and B show cumulative data of four independent experiments. (C) Spleens and peripheral blood cells from high expressing huTLR8Tg chimeras or WT controls were harvested, and co-stimulatory molecule expression was analyzed on CD11c$^+$ cells in spleens (top) and blood (middle) and splenic CD11b$^+$ cells (bottom). CD11c were gated based on the expression of MHC-class I. CD11b$^+$ cells were gated on CD11c^{neg} cells and on the expression of MHC class I. H2b (C57BL/6)-positive cells expressing huTLR8 (black line) were compared with H2b-negative cells (BALB/c, red line) not expressing huTLR8 in the same animal. Blue line, WT animal. CD11b^{pos} CD11c^{neg} monocytes in the spleen were gated on the expression of MHC-class I. H2b (C57BL/6)-positive cells expressing huTLR8 (black line) are compared with H2b-negative cells (BALB/c, red line) not expressing huTLR8. Plots are representative of at least three independent experiments. (D) Expression of co-stimulatory molecules in CD11c from spleens of TLR8TgCL12>B6.SJL (black line) or C57BL/6 (red line) chimeric mice. Plots are representative of at least three independent experiments. (E) CD11c cells were purified from spleens of TLR8TgCL12>B6.SJL (TLR8DC) or C57BL/6>B6.SJL (WTDC) chimeric mice. The CD11c$^+$ cells were loaded with $Ova_{323-339}$ and used to stimulate OT-II T cells at the indicated DC:T cells ratio. One representative experiment of two is shown. *, P ≥ 0.05; **, P ≥ 0.01.

Published November 25, 2013

Table 1. Frequencies of leukocytes in huTLR8Tg chimeras

	Spleen		Blood	
	WT	huTLR8Tg	WT	huTLR8Tg
Total spleen cell number	$6 \times 10^7 \pm 0.2$	$4 \times 10^7 \pm 0.8^a$		
	%	%	%	%
$CD3^+CD4^+$ T cells	23 ± 0.7	19 ± 1.4	17 ± 1.2	9 ± 1.5[b]
Naive ($CD62L^{hi}$ $CD44^{low}$)	72 ± 0.5	55 ± 4.6[c]	72 ± 3.5	53 ± 8.3[a]
Effector ($CD62L^{hi}$ $CD44^{hi}$)	5.2 ± 0.4	6 ± 0.77	2 ± 0.5	3 ± 0.7
Effector memory ($CD62L^{low}CD44^{hi}$)	18 ± 0.7	35 ± 5.5[c]	18 ± 3.6	39 ± 8[a]
$CD3^+CD8^+$ T cells	12 ± 0.5	10 ± 0.7	9.3 ± 1.7	6 ± 1.1
Naive ($CD62L^{hi}$ $CD44^{low}$)	74 ±1.1	58 ± 4.8	74 ± 2.7	46 ± 4[b]
Effector ($CD62L^{hi}$ $CD44^{hi}$)	16 ± 0.7	15 ± 2.2	11 ± 1.6	23 ± 3.3[b]
Effector memory ($CD62L^{low}CD44^{hi}$)	7 ± 0.4	23 ± 6[c]	11 ± 3.3	24 ± 3.6[a]
T reg ($CD4^+$ $CD8^+$ $FOXP3^+$)	1.5 ± 0.3	2 ± 0.4	2 ± 0.3	2 ± 0.4
$CD19^+$ B cells	49 ± 1.7	47 ± 3.2	48 ± 4	38 ± 4[a]
Monocytes ($CD11b^+Ly6G^-F4/80^+$)	2 ± 0.2	3 ± 0.3	5 ± 0.6	11 ± 1.4[b]
Neutrophils ($CD11b^+Ly6G^+F4/80^-$)	1 ± 0.14	3 ± 0.4[c]	6 ± 1	20 ± 6[c]
$CD11c^+$ DC	4 ± 0.3	3 ± 0.4	3 ± 0.5	4 ± 0.5

Data are from TLR8 Tg clone 12 sacrificed when moribund (50–120 d old) and matching C57BL/6 WT mice; *n* = 17/per group (mean ± SEM). Main cell populations are represented as percentage of total live spleen or blood cells. Subpopulations are in bold.
[a]$P \leq 0.05$.
[b]$P \leq 0.01$.
[c]$P \leq 0.001$.

Altered expression of TLR8 in patients with systemic arthritis disease

TLR8 has a very distinct expression pattern as compare to TLR7 and TLR9 in human blood, it is expressed in monocytes, mDCs, and neutrophils while TLR7 and TLR9 are coexpressed, primarily on B cells and PDC (Fig. 9 A; Hattermann et al., 2007; Forsbach et al., 2008; Janke et al., 2009). Gene expression profiling of stimulated human PBMCs reflected these differences in cellular distribution. PBMCs stimulated by a specific TLR8 ligand showed high levels of proinflammatory genes, including IL-6, IFN-γ, IL-1, IL-23 and TNF, as well as chemokines involved in inflammatory responses. In contrast to TLR7 and TLR9, TLR8 ligand did not induce type 1 IFN-regulated gene, likely due to its lack of expression on PDC (Fig. 9 B). Thus TLR8-induced response is significantly different from the one induced by TLR7 (Fig. 9 C).

As we observed that TLR8 can exacerbate arthritis in the murine arthritis model (Fig. 8), we measured the level of expression of TLR8 in patients with arthritis and found an increased level both in patients with Systemic onset juvenile arthritis (SoJIA) and its adult equivalent, Still's disease (Fig. 10 A). Patients affected by these diseases have a dysregulated production of IL-1β and can be successfully treated with inhibitors of the IL-1 pathway. The triggering factors and the innate receptors responsible for this increase in IL-1β are, however, not yet defined (Mellins et al., 2011; Pascual et al., 2005). TLR8 mRNA expression was significantly higher in blood cells of both SoJIA and Still's disease (Fig. 10 A). Furthermore, the expression of TLR8 mRNA correlated positively with the levels of IL-1β transcripts (Fig. 10 B) in these patients, which was not the case with mRNA for TLR7 or TLR9 (Fig. 10 C). The correlation of both IL-1β production and disease activity with TLR8 expression is further supported by the normalization of TLR8 mRNA in SoJIA patients treated with the IL-1 receptor antagonist, Anakinra (Fig. 10 A, cohort 2). A similar increase was found in purified monocytes from SoJIA patients with active disease (Fig. 10 D) but not in neutrophils (not depicted), suggesting that difference in TLR8 expression level in whole blood is not simply a reflection of altered peripheral blood populations. As patients with systemic arthritis have chronic overexpression of proinflammatory cytokines, we assessed the impact of IL-1β, IL-6, TNF, and IFN-γ on TLR8 expression. None of these cytokines had a significant effect on huTLR8 expression both in human PBMCs (Fig. 10 E) and in PBMCs from TLR8TgCL8 mice (Fig. 10F). Taken altogether, these data indicate that TLR8 is overexpressed in patients with systemic arthritis and suggest that the signaling through this receptor may play a role in the disease pathogenesis. This is particularly relevant in the context of our observations in the human TLR8 transgenic animals.

DISCUSSION

Considerable understanding has been developed in the past decade about the potential deleterious consequences for self-nucleic acids recognition by TLR7 and 9 and selective antagonists of these two receptors are now being tested in clinical trials for the treatment of various autoimmune disorders (Barbalat et al., 2011; Guiducci et al., 2009). Despite some

Published November 25, 2013

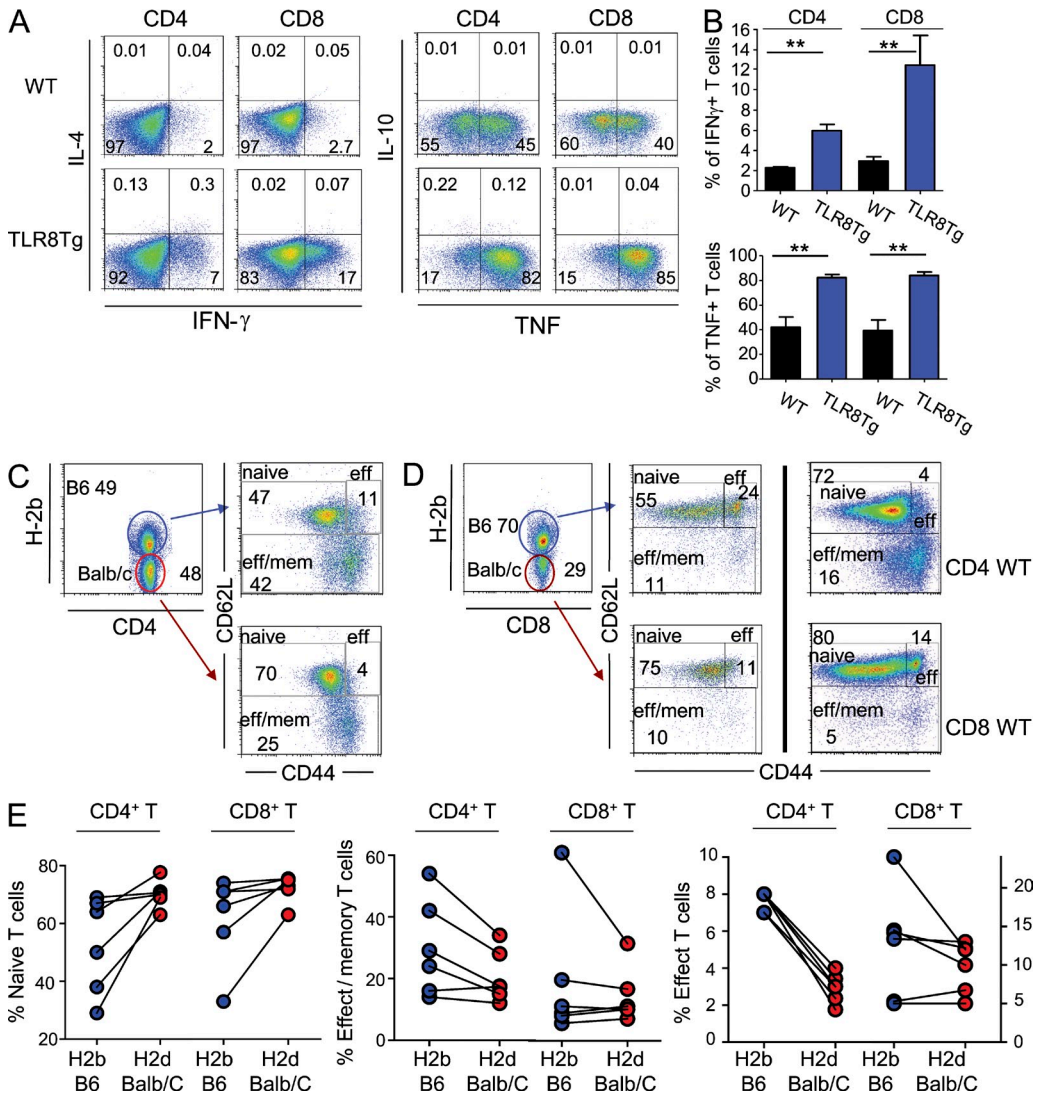

Figure 5. T cell compartment is highly activated in huTLR8Tg mice. (A and B) Splenocytes from either high expressing TLR8TgCL12 chimeras in which at least 95% of the hematopoietic compartment was H2b^{pos} (C57BL/6) or C57BL/6 WT mice were stimulated in vitro for 2 h with PMA and ionomycin. Percentages of CD4 and CD8 T cells producing TNF and IFN-γ were assessed by flow cytometry. (A) Representative dot plots. (B) Quantitation of data in A from one representative of three independent experiments (n = 3 mice; mean ± SEM). (C and D) TLR8TgCL12 chimeras were sacrificed and spleens were harvested. (C) CD3$^+$CD4$^+$ and (D) CD3$^+$CD8$^+$ T cells were gated based on the expression of MHC class I. (D) Right panel shows representative dot plot of CD3$^+$CD4$^+$ and CD3$^+$CD8$^+$ from C57BL/6 WT mice from three independent experiments. (E) Quantitative intramouse data showing naive, effector memory, and effector T cells population for both haplotypes (huTLR8Tg in red, WT in blue). **, P ≥ 0.01

significant species differences between rodents and human in TLR expression patterns, much of this knowledge has been gained from studies performed in mouse models of autoimmune disease or gene-targeted mice (Christensen et al., 2006; Deane et al., 2007; Barrat et al., 2007; Ewald et al., 2011; Mouchess et al., 2011; Walsh et al., 2012). TLR8 belongs to the same family as TLR7 and TLR9, but its role in disease has yet to be elucidated due to the lack of an appropriate animal model to study its function in vivo. Interpretation of the role of TLR8 in inflammation has relied mostly on work performed on mouse TLR7, which shares with human TLR8 its ability to detect ssRNA in the endosome but has a different cellular distribution and some different ligand specificity in vitro (Forsbach et al., 2008) and likely in vivo. We showed that activation of the TLR8 signaling pathway in human blood results in a predominant proinflammatory gene signature, whereas activation of TLR7 is associated with a type I IFN response, demonstrating that the cellular distribution of these two receptors is an essential element of their biology. In addition, understanding the role of TLR8 has proven difficult as the mouse TLR8 seems to differ from its human orthologue due to the lack of 5 aa that are key for RNA recognition.

Here, we generated mice expressing functionally active huTLR8 with a similar expression pattern to that in human

Published November 25, 2013

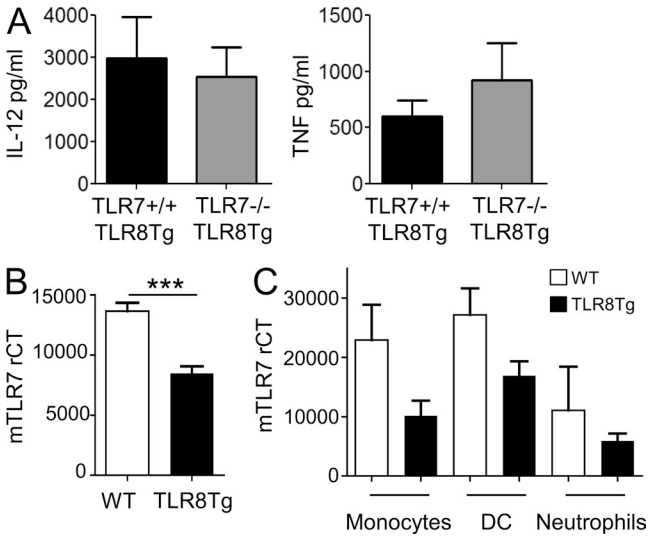

Figure 6. Human TLR8 can function in absence of mouse TLR7, but it regulates its expression levels. (A) 5×10^5 PBMCs from TLR7$^{+/+}$ TLR8TgCL8 line and from TLR7$^{-/-}$ TLR8TgCL8 were stimulated with a specific RNA-based TLR8 agonist, ORN-8L, supernatants were harvested at 24 h and assayed for cytokines levels by ELISA; One representative experiment of three is shown. $n = 4$; mean ± SEM. (B) Mouse TLR7 expression was evaluated by TaqMan in spleens of TLR8TgCL12 ($n = 22$) and TLR8TgCL23 ($n = 4$) chimeras and WT C57BL/6 ($n = 30$; mean ± SEM). (C) Cellular subsets were isolated from spleens of TLR8TgCL12>B6.SJL mice or with C57BL/6>B6.SJL, as described in the Materials and methods. Gene expression of mouse TLR7 was evaluated by TaqMan. (B and C) Cumulative data from three independent experiments; $n = 5$–10; mean ± SEM; ***, $P \geq 0.001$.

leukocytes. The severity of the specific phenotypes closely correlated with the expression levels of huTLR8 and relatively small difference in its expression lead to inflammation in multiple organs.

Pancreas failure was likely the primary cause of death of huTLR8Tg chimeras. The histological features of the involved pancreas showed similarity with primary autoimmune pancreatitis in humans (AIP), including a dense leukocyte infiltration consisting of T cells, macrophages, and neutrophils associated with large areas of interstitial fibrosis (Zandieh and Byrne, 2007). Interestingly, huTLR8Tg mice develop extrapancreatic lesions in organs often affected in AIP patients, including salivary glands inflammation, glomerulonephritis, and inflammation in the portal area of the liver (Finkelberg et al., 2006; Zandieh and Byrne, 2007). Although it is difficult to accurately compare the levels of huTLR8 in these transgenic animals to the levels in human cells, our data clearly demonstrate that the inflammatory status is directly proportional to level of huTLR8 expression. One may predict that in humans, increased level of huTLR8 expression or possibly improper intracellular compartmentalization might lead to loss of immune tolerance.

huTLR8Tg chimeras developed spontaneous joint inflammation and the stable line expressing lower huTLR8 levels is more susceptible to collagen-induced arthritis as compared with syngeneic WT mice. It is interesting that the difference with syngeneic animals only occurs once disease is established (Fig. 7 C). A possible scenario is that the initial process of joint injury induces the release self-RNA–peptide complexes (Ganguly et al., 2009). Infiltrating or resident macrophages would respond to this self-RNA through huTLR8, but not mouse TLR8, leading to increased production of proinflammatory mediators, which further enhance the disease process in transgenic mice. This suggests that huTLR8 is not involved in the initial phase of disease, but becomes a key player in the maintenance phase. In patients with systemic arthritis, we found an increased level of TLR8 in PBMCs of SoJIA patients and in patients with Still's disease. Such increase could be caused by differences in cellular composition, but we observed a similar increase in purified monocytes from patients and a significant correlation with IL-1β. Interestingly, TLR8 expression levels is not regulated by IL-1β or IL-6, thought to be a primary abnormality associated with systemic arthritis, in what could have been a positive feedback loop in these patients suggesting a different mechanism leading to TLR8 increased expression. Our observations using the transgenic mice have highlighted the dramatic impact of a slight increase in TLR8 expression on the overall state of inflammation in vivo. The similar high expression level of TLR8 in patients with arthritis thus argues for a role of this receptor in the pathogenesis of the disease.

We took advantage of the coexistence in the blood of the chimeras of WT H2d cells and H2b-TLR8-bearing cells and demonstrated a selective activation of huTLR8-expressing DCs and monocytes, indicating that huTLR8 signaling exerts a cell-intrinsic effect. A possible contributor to the DC and monocyte activation in huTLR8Tg chimeras are the elevated levels of anti-RNP Ab (Fig. 2 E), which can activate the receptor in virtue of their high affinity for ssRNA (Vollmer et al., 2005). However, DCs and monocytes are similarly activated in BM-transplanted mice (Fig. 4, E and F) which have undetectable levels of anti-RNP (data not shown), suggesting that these cells sense other type of RNA ligands or at least that anti-RNP IC are not exclusively responsible for their activation. In the majority of huTLR8Tg chimeras, huTLR8-DC activation is paralleled by a preferential activation of H2b T cells. Notably, in few of the very sick animals analyzed, we found over 80% of T cells with an effector memory phenotype, and in these cases both H2b cells and H2d T cells were activated to a similar extent (data not shown). Thus, a process initially confined to cognate activation of T cells by huTLR8-DC can ultimately involve noncognate activation of T cells once the response reaches certain intensity. In the transgenic mice, activated DCs and monocytes infiltrating the pancreas, might be exposed to self-antigens in a highly stimulatory environment which can lead to T cell activation. It is therefore possible that the inflammatory process, initially geographically restricted to the pancreas or another organ, would results to a rapidly progressing disease in other organs in a T cell dependent manner. Construction of more sophisticated models to be able to simultaneously track TLR8 expression

Published November 25, 2013

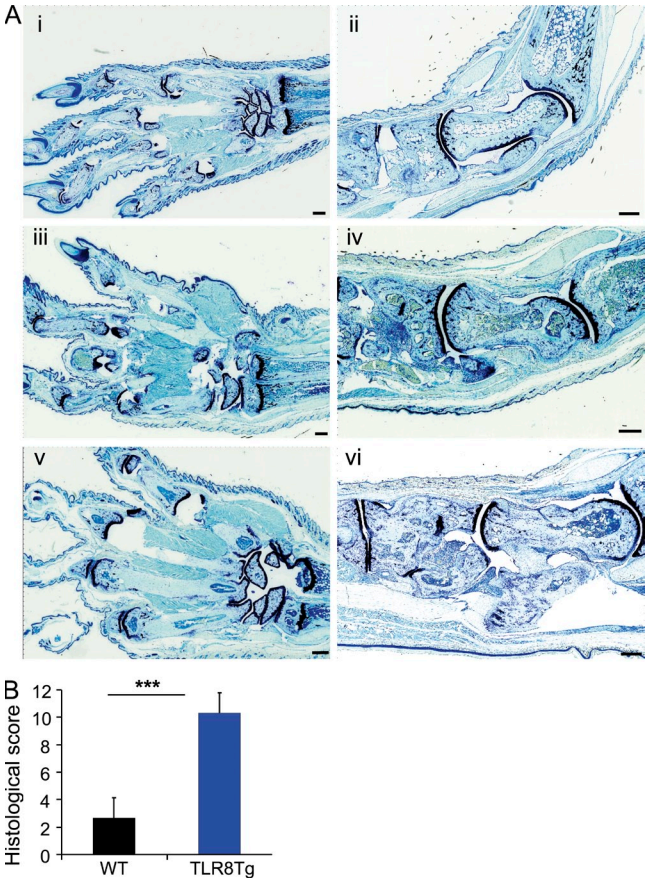

Figure 7. Spontaneous arthritis develops in high expressing huTLR8Tg mice. (A) Chimera mice from TLR8TgCL12 ($n = 6$) and C57BL/6 CTLR animals ($n = 6$) were euthanized 90 d after the birth, and paws and joints were fixed, sectioned, and stained with toluene blue. Representative sections of paws from WT mice (i) and TLR8TgCL12 mice (iii and v) and joints from WT (ii) and TLR8TgCL12 mice (iv and vi). (B) The histological changes, degree of inflammation, and cartilage damage were evaluated by a pathologist in a blinded fashion and scored 1–5 as followed: 1, minimal; 2, mild; 3, moderate; 4, marked; 5, severe. Two paws and two ankles were evaluated for each animal and the scores were summed to obtain the histological disease score. ***, $P \geq 0.001$. Bar, 300 mm.

and activation in the early phase of the disease are required to clarify this point.

Although it is well known that huTLR8 recognize and gets activated by ssRNA, a key question is to better understand which ligands activate the receptor in vivo to induce such a dramatic break of tolerance and where does this happen first. The receptor is not constitutively active as spontaneous production of cytokines was not observed after in vitro culture of PBMCs from any of the transgenic lines. The sensing of extracellular RNA is also unlikely since in transgenic animals, huTLR8 required receptor proteolysis in the endosome for its activity. As shown recently for TLR9, the proteolytic processing in the endolysosomal compartment is an essential mechanism to avoid recognition of extracellular self-DNA (Ewald et al., 2011; Mouchess et al., 2011) and mice expressing a form of TLR9 which no longer requires receptor proteolysis for activation, sense extracellular self-DNA and die of a fulminating form of anemia (Mouchess et al., 2011). In addition, there is no obvious basis for chemical differences between mouse and human RNA and it is thus unlikely that the receptor is activated by a specific mouse RNA ligands not present in humans. However, we cannot exclude that sequence motifs preferentially recognized by huTLR8 might be more represented in mice than in humans. Another possibility is that huTLR8 is activated by virus or microbe RNAs not present in humans. However, in mice transplanted with huTLR8Tg–bone marrow, the disease severity was greatly accelerated, a phenomena that likely resulted from the abundance of self-RNA released as a consequence of the massive cell-death induced by the radiation, rendering the hypothesis of a specific mouse pathogens less plausible.

Previous work has shown that increased expression of TLR7 is sufficient, independently of any other genetic lesions, to break tolerance in mice (Deane et al., 2007; Walsh et al., 2012). Similarly, transgenic mice for the D34 mutation in the chaperone protein Unc93B1 preferentially transport TLR7 versus TLR9 in the signaling endosome and develop autoimmunity (Fukui et al., 2011). In both cases, mice developed a massive lymphoproliferation. Surprisingly, we did not observe myeloid cell expansion or any signs of lymphoproliferation in the huTLR8Tg mice. On the opposite, lymphopenia not lymphoproliferation characterized these animals, suggesting a profound difference between TLR8 versus TLR7.

Other disease traits significantly differentiate the consequence of increased huTLR8 versus TLR7 signaling in mice. TLR7Tg mice develop glomerulonephritis, liver necrosis, and a severe form of anemia, whereas pancreas, joints, and salivary glands are not affected, rendering the glomerulonephritis aspect of the diseases as probably the only common trait between the two models. In the TLR7Tg mice, absence of B cells is sufficient to abrogate the entire spectrum of symptoms, including DC activation and expansion, demonstrating that excessive TLR7 signaling in B cells drives the disease in this model. In the huTLR8Tg mice, it is unlikely that B cells play a similar central role to the disease. In fact, B cells in these mice express very low huTLR8 and don't expand or infiltrate the involved organs. The increased levels of nucleic acid–specific antibodies in the huTLR8Tg mice, however, suggest a break of B cell tolerance in both DNA- and RNA-binding proteins, but this phenomena happened late in the disease pathogenesis in the chimeras and was absent in the BM-transplanted animals. Mechanistically, it is more likely that DCs and macrophage activation plays the critical step in the initiation of the inflammatory process by producing proinflammatory cytokines such TNF, IL-1β, and IL-6, which can mediate end organ damage, and promoting Th1 priming and differentiation of CD8 T into IFN-γ/TNF-producing cells. Although the overexpression of either TLR7 or huTLR8 in mice leads to a strong inflammatory response and disease symptoms, the phenotype of the mice is thus drastically different. This is quite puzzling, as both receptors recognize

Published November 25, 2013

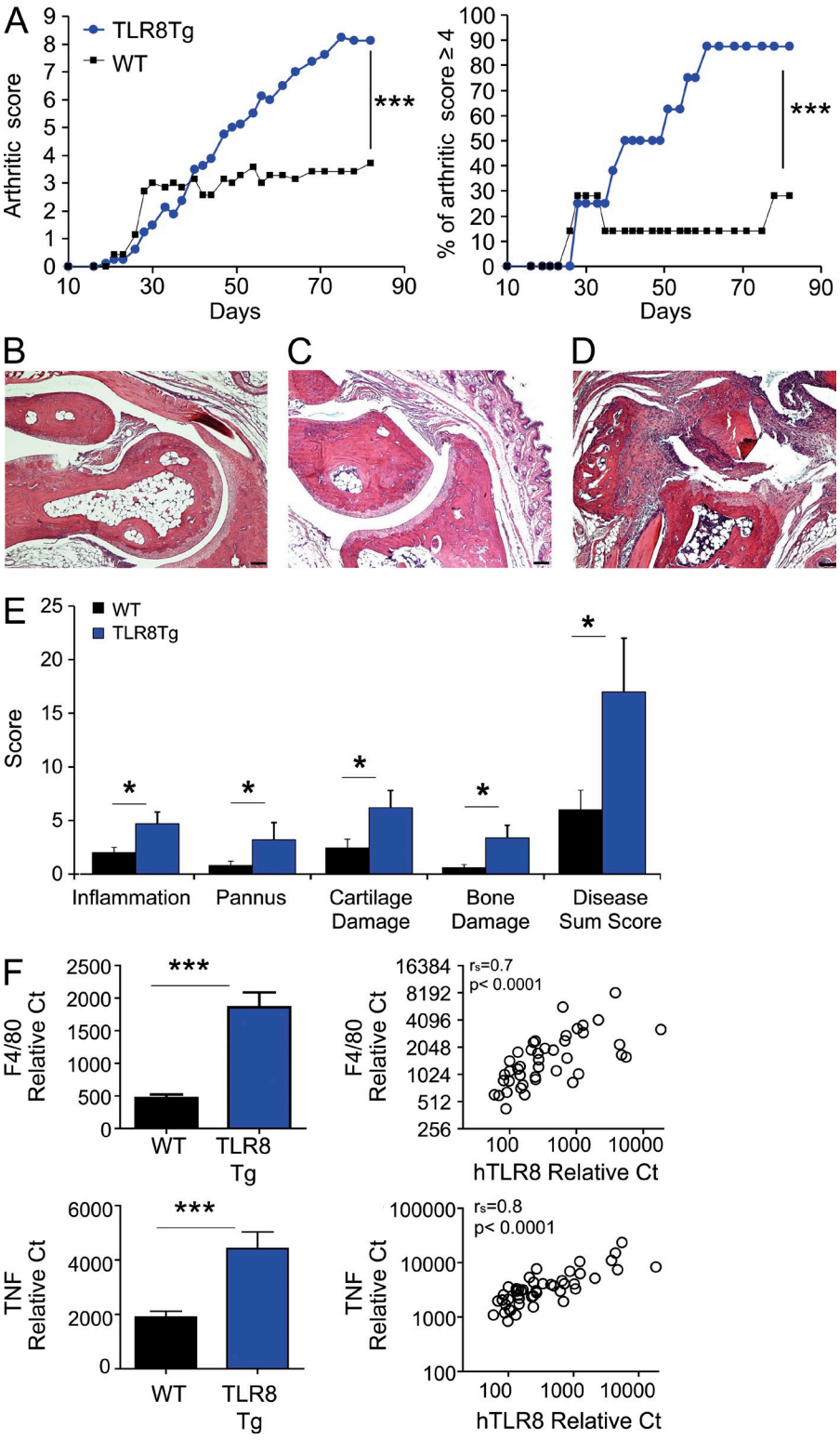

Figure 8. huTLR8Tg mice have increased susceptibility to arthritis. (A) TLR8TgCL8 line and age-matched WT controls (left) were immunized with collagen and disease score was measured. Total arthritis score (left) and percentage of mice with clinical score equal or more than four (right) in the two strains is shown. One representative experiment (n = 10 mice per group) of 4 is shown (40 mice total per group). Statistical significance was evaluated with a two-way ANOVA test. (B– D) Representative sections (hematoxylin and eosin stained) of normal (B), WT (C), and TLR8TgCL8 (D) joints, sacrificed 80 d after CIA induction. (E) Cumulative data from histopathological evaluation in B–D. Animals were sacrificed at day 80 after CIA induction and joints of hind paws were fixed, sectioned, and stained with H&E. The four histological changes (inflammation, pannus formation, cartilage, and bone damage) were evaluated by a pathologist in a blinded fashion as described in the Materials and methods. Table shows cumulative data from 2 independent experiments, TLR8TgCL8 (n = 16) or WT (n = 15); mean ± SEM; a = $P \leq 0.05$ (F) Expression of F4/80 and TNF in the joints of TLR8TgCL8. The two front joints of each animal (WT or huTLR8Tg) were used to prepare RNA and F4/80, and TNF expression was evaluated by TaqMan. Animals were sacrificed 80 d after CIA induction. Number of joints 46 per group (mean ± SEM); data are cumulative of two independent experiments. P-values were calculated using a nonparametric correlation test (Spearman). *, $P \geq 0.05$; ***, $P \geq 0.001$. Bar, 100 µm.

ssRNA and one would predict a similar inflammatory response linked to increase expression. Some of the key differences were the targeted organs but also the cellular response. This could be caused by intrinsic differences in the biology of these receptors but it is tempting to postulate that the cellular distribution of these receptors is the key differentiation element. In the huTLR8Tg mice, TLR8 is restricted to myeloid cells, whereas TLR7, in addition to myeloid cells, is also present in B cells, T cells, and PDCs. The cellular distribution of TLR8 in the transgenic mice is similar to the human, at

Published November 25, 2013

A

	TLR8	TLR7	TLR9
monocyte	36282±9282	1983±428	630±130
m DC	50004±13940	9439±2379	78±25
neutrophils	41288±5390	829±255	1972±163
B cells	55±11	2210±151	2325±494
PDC	60±26	6009±372	9288±1625
CD4+CD25-	23±4	79±3.5	271±35
CD4+CD25+	60±24	237±36	463±54

B

Inflammatory mediators

Med	TLR7L	TLR8L	TLR9	Gene
1	95	297	29	IL6
1	12	121	15	IFNG
1	11	118	1	IL1F9
1	18	50	2	IL19
1	20	34	16	IL1RN
1	8	27	7	IL1A
1	7	23	2	IL10
1	4	21	3	TNF
1	4	10	3	IL2RA
1	3	9	1	TNFSF9 (41BB-L)
1	9	8	4	IL15RA
1	4	8	2	IL27
1	6	7	2	TNFAIP6
1	3	5	1	TGF-A
1	4	4	3	IL1B
1	2	4	2	TNFRSF18 (GITR)
1	6	3	11	TNFSF10 (TRAIL)
1	3	0.5	3	TNFSF13B (BAFF)

Chemokines

Med	TLR7L	TLR8L	TLR9	Gene
1	22	280	6	CCL20
1	5	38	2	CCL14
1	15	33	6	CCL3L1
1	12	15	6	CCL3
1	12	15	6	CCL3
1	11	13	6	CXCL9
1	1	13	1	CXCL2
1	4	8	2	CXCL1
1	4	8	2	CXCL1
1	8	7	7	CCL2
1	8	5	13	CXCL10
1	3	5	3	CXCL5
1	3	4	1	CCL1
1	33	3	36	CCL8
1	3	3	1	CCL19

Type I IFN regulated transcripts

Med	TLR7L	TLR8L	TLR9	Gene
1	10	3	15	IFIT1
1	10	5	13	IFIT3
1	8	5	9	ISG15
1	5	3	8	IFIT2
1	8	3	7	OAS1
1	7	4	7	IFI44
1	9	4	6	OAS3
1	12	5	5	IFI6
1	5	3	5	OASL
1	5	3	4	MX2

C

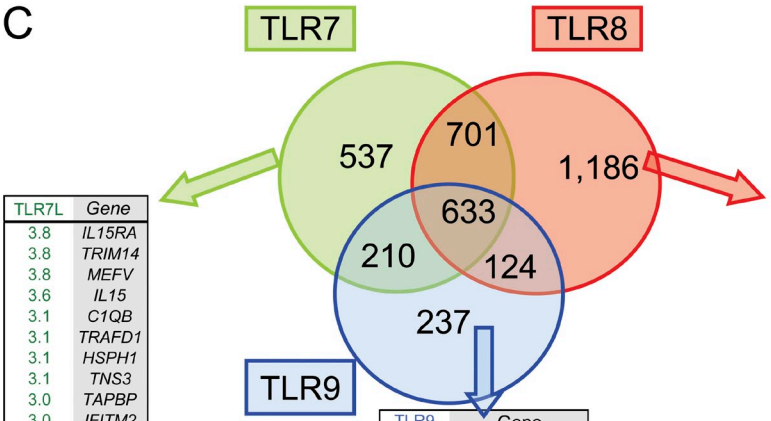

TLR7L	Gene
3.8	*IL15RA*
3.8	*TRIM14*
3.8	*MEFV*
3.6	*IL15*
3.1	*C1QB*
3.1	*TRAFD1*
3.1	*HSPH1*
3.1	*TNS3*
3.0	*TAPBP*
3.0	*IFITM2*
2.9	*PSMB9*
2.9	*TAP2*
2.9	*CXCL6*
2.6	*PRF1*
2.5	*CASP7*
2.4	*TRADD*
2.2	*TNFAIP2*

TLR9	Gene
8.6	IFNA7
6.3	IFNA2
6.3	IFNA16
4.9	IFNA10
3.1	IFNA21
2.9	IFNA13
2.4	SPIB
2.2	DDX19-DDX19L
2.2	IFNW1
2.1	TLR2
2.0	IFNA14

TLR8L	Gene
12.6	CXCL2
10.2	IL24
8.5	G-CSF3
6.6	IL1R1
4.9	TNFRSF21
4.3	IL2RA
4.2	NLRP3
3.5	MMP10
3.3	RNY5
3.2	STAT4
3.1	TNFRSF4
2.8	RNU1-5
2.5	RNU4ATAC
2.7	IL23A
2.7	CD83
2.6	IL8
2.4	IL4R
2.3	NCRNA00092
2.3	SNORA57
2.2	RNU11
2.3	ICOS
2.1	TNFSF14
2.0	IL1F5

Figure 9. TLR8 signaling induces a discrete panel of proinflammatory genes in humans. (A) Cellular subsets were isolated from whole blood of healthy donors and expression of TLR7, 8, and 9 was analyzed by TaqMan assay. Relative Ct of the genes is shown in the table. Cumulative data from at least four independent donors is shown (mean relative CT ± SEM). (B and C) 4×10^5 PBMCs from four healthy donors were stimulated for 6 h with or without TLR7L (CL264; 5 µg/ml), TLR8L (ORN8L; 200 µg/ml), and TLR9L (C274; 0.3 µM). Stimulated samples from each donor were normalized to their own unstimulated control (in medium only). Transcripts over- and underexpressed at least twofold were selected. In B, representative genes are grouped by family; mean fold up-regulation is shown for each ligand. In C, Venn diagram depicts the overlap between TLR7, 8, and 9 ligands for all genes differentially expressed in the three conditions. (C) List of genes specifically up-regulated by TLR8 ligation (right), TLR7 ligation (left), and TLR9 ligation (middle). Notably, a class of TLR8-specific genes (highlighted in orange) belongs to a family coding for highly conserved RNA molecules component of RNP, which constitute potent TLR8 activators (Vollmer et al., 2005).

Published November 25, 2013

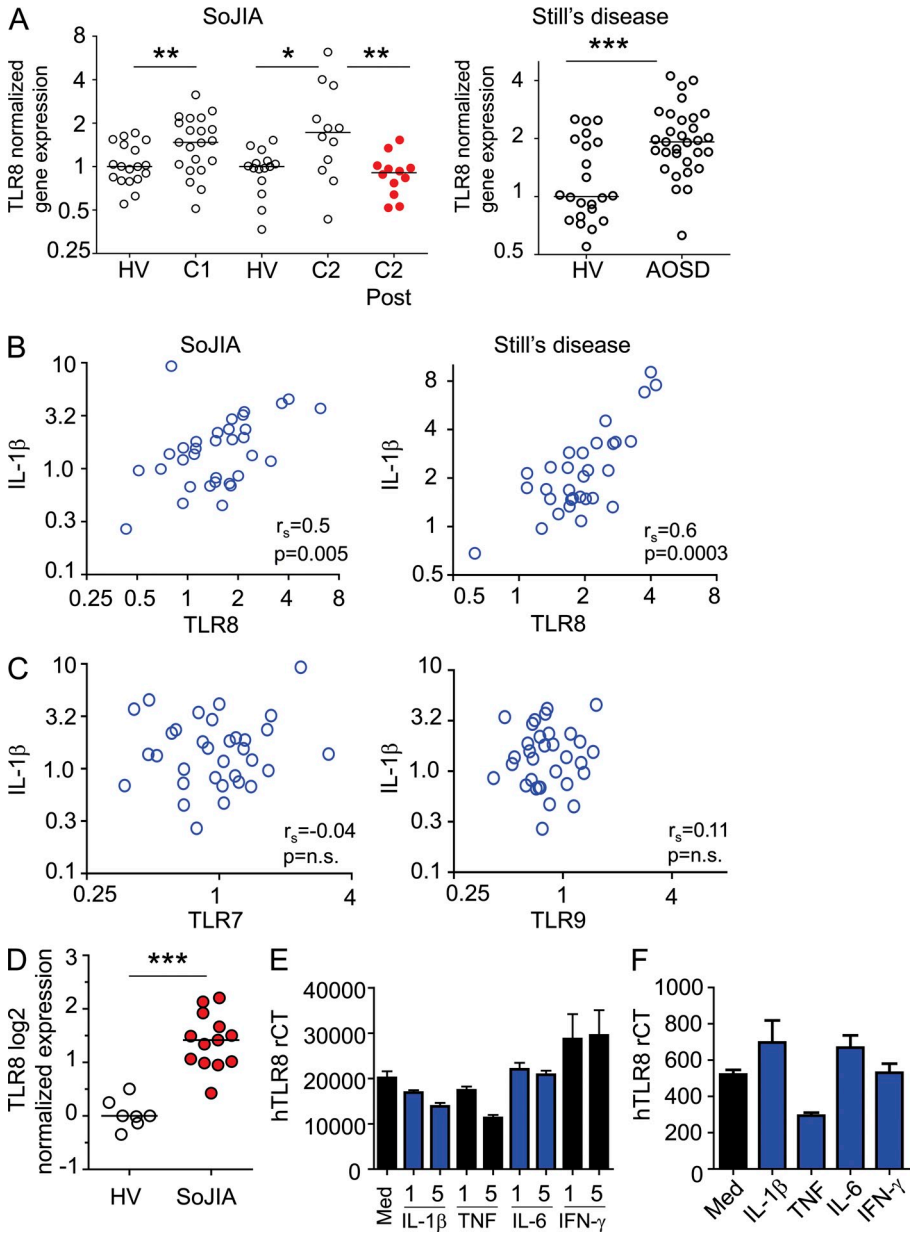

Figure 10. The TLR8 pathway is dysregulated in systemic arthritis patients. (A) Expression of TLR8 in the blood of systemic-onset juvenile arthritis patients (SoJIA; two cohorts; left; $n = 33$) and Still's disease patients (right; $n = 31$). The level of huTLR8 in each of the cohorts was normalized to the level of the gene in healthy volunteer cohorts (HV). Cohort 2 of the SoJIA patients was treated with Anakinra (IL-1 receptor antagonist), and levels of huTLR8 gene expression was compared before and after treatment (red dots). (B) Expression levels of TLR8 were plotted against blood levels of IL-1β of SoJIA (cohort 1 and 2 combined) and Still's disease. (C) Similarly to C levels of TLR7 and TLR9 are shown for SoJIA (cohort 1 and 2 combined). In B and C, p-values were calculated using a nonparametric correlation test (Spearman). (D) TLR8 expression levels in purified monocytes from SoJIA patients with active disease. Human PBMCs (E) or mouse PBMCs from huTLR8TgCL8 mice (F) were cultured for 16 h with 1 ng or 5 ng/ml (for human PBMCs) or 5 ng/ml (mouse PBMCs) of the indicated cytokines, and levels of huTLR8 expression were assessed by TaqMan. The experiments were conducted twice with a total of eight human donors (E) and nine mice (F). Shown is mean ± SEM. *, $P \geq 0.05$; **, $P \geq 0.01$; ***, $P \geq 0.001$.

least in the hematopoietic compartment, which makes the mice a relevant model to study TLR8 biology. Mouse TLR8 does not deliver an activation signal but is critical to control mTLR7 expression and as such prevents the occurrence of TLR7-driven autoimmunity in mice (Demaria et al., 2010). In line with these findings, we observed a marked reduction in mTLR7 expression in cellular subsets expressing huTLR8. This could constitute a mechanism to prevent the simultaneous expression of both receptors behind a certain threshold level. The presence of TLR7 in myeloid cells in mice indeed suggests that it compensates for the lack of a functional TLR8 in mice, whereas in humans, both receptors are expressed in different

Published November 25, 2013

cell types and induce a qualitatively different inflammatory response (Fig. 9).

In conclusion, using novel human TLR8 transgenic mice, we have identified TLR8 as a key player in autoimmune inflammation in human diseases and defined a link between TLR8 and arthritis both in mouse models but also in patients. Our data provide for the first time some clear understanding of the difference in the in vivo biology of TLR7 versus TLR8 and argue for the importance of restricting excessive TLR7 or TLR8 response in vivo pointing to the existence of sophisticated mechanisms controlling level of recognition of self-RNA in endosomes by these two receptors. We believe that we have uncovered the role of TLR8 in human autoimmune inflammatory diseases, which identifies TLR8 as a key potential target for clinical development

MATERIALS AND METHODS

Reagents. TLR8 agonist stabilized immunomodulatory RNA (ORN8-liter; 5′-M2UGCUGCUUGUG-/glycerol/-GUGUUCGUCGUM2-5) was previously described (Lan et al., 2007) and synthetized by Chemgenes Corporation. Small molecule TLR7 agonists CL264 was from InvivoGen.

Transgenic mice and bone marrow chimeras. Transgenic mice expressing human TLR8 were generated using generated using BAC/ES technologies (Sparwasser and Eberl, 2007). A human BAC containing TLR8 was transfected into C57BL/6NTac ES cell line, and four clones were chosen with a range of inserted human TLR8 in the genome and used to generated transgenic mice expressing TLR8. The level of human TLR8 expression in whole blood or splenocytes of transgenic animals was assessed by real-time quantitative PCR analysis.

For bone marrow chimeras, C57BL/6SJL (CD45.1) female mice were irradiated with two doses of 450 rad at 3-h intervals from a cesium source and reconstituted 4 h later with 1.7×10^6 bone marrow cells from transgenic chimeras or WT C57BL/6 (CD45.2). Mice were kept on antibiotics (neomycin sulfate) for 3 wk. Flow cytometry analysis on blood was used to evaluate level of chimerism using anti-CD45.2 and anti-CD45.1 antibodies (BD). Animal experiments were conducted in Murigenics. All animal experiments were approved by the institutional animal care and use committee of Murigenics (IACUC), in conformity with the Guide for the Care and Use of Laboratory Animals (NRC).

Hematological and serological analysis. Mouse blood sample were obtained from retro orbital bleeding and hematological parameters were assessed using the Heska CBC-Diff Veterinary Hematology System. Nucleic acids ds-DNA autoantibodies were evaluated with commercially available ELISA kits (Alpha Diagnostic). For anti-dsDNA assessment, sera were diluted 1:100 or 1:30, respectively. For anti-RNP, sera were diluted 1:100 and assessed as previously described (Barrat et al., 2007).

Collagen-induced arthritis model (CIA). TLR8TgClone8 mice and WT (C57BL/6; littermate controls not expressing the transgene) were immunized per a published immunization schedule and protocol (Campbell et al., 2000). Animals were assessed for redness and swelling of the four limbs and the cumulative score of each mouse was the sum of the score obtained for each limb. The Clinical Score Guidelines were as follows: 0, normal; 1, mild, but definite redness and swelling of the ankle or wrist, or apparent redness and swelling limited to individual digits, regardless of the number of affected digits; 2, moderate redness and swelling of ankle of wrist; 3, severe redness and swelling of the entire paw including digits; and 4, maximally inflamed limb with involvement of multiple joints.

Pathology. The biopsy specimens were fixed in formalin and embedded in paraffin and sections were stained with hematoxylin-eosin. Blinded evaluation of the liver, kidney, salivary gland, lung, brain, heart, and pancreas was conducted by a pathologist during the course of the study. Multiple organs sections were evaluated for each organ. Inflammation was scored 1 to 4 as follow: 1, minimal; 2, mild; 3, moderate; 4, marked. Statistical significance among groups was calculated with a Mann-Whitney *U* test with p-values comparing chimeric mice to age-matched CTRL B6 animals. P-values were considered statistically significant at $P \leq 0.05$. For evaluation of arthritic joints in the CIA model, both front and hind limbs from each animal were fixed, sectioned, and stained with H&E and toluidine blue, and the wrist and ankles were scored for pathological changes. The four histological changes (inflammation, pannus formation, cartilage, and bone damage) were evaluated in a blinded fashion with the following criteria: Inflammation: 0, normal; 1, minimal infiltration of inflammatory cells in synovium and periarticular tissue of affected joints; 2, mild infiltration; 3, moderate infiltration with moderate edema; 4, marked infiltration affecting most areas with marked edema; 5, severe diffuse infiltration with severe edema. Pannus: 0, normal; 1, minimal infiltration of pannus in cartilage and subchondral bone of marginal zone; 2, mild infiltration of marginal zone with minor cortical and medullary bone destruction in affected joints; 3, moderate infiltration with moderate hard tissue destruction in affected joints; 4, marked infiltration with marked destruction of joint architecture, affecting most joints; 5, severe infiltration associated with total or near total destruction of joint architecture, affects all joints. Cartilage damage: 0, normal; 1, minimal to mild loss of toluidine blue staining with no obvious chondrocyte loss or collagen disruption in affected joints; 2, mild loss of toluidine blue staining with focal mild (superficial) chondrocyte loss and/or collagen disruption in affected joints; 3, moderate loss of toluidine blue staining with multifocal moderate (depth to middle zone) chondrocyte loss and/or collagen disruption in affected joints; 4, marked loss of toluidine blue staining with multifocal marked (depth to deep zone) chondrocyte loss and/or collagen disruption in most joints; 5, severe diffuse loss of toluidine blue staining with multifocal severe (depth to tide mark) chondrocyte loss and/or collagen disruption in all joints. Bone resorption: 0, normal; 1, minimal, small areas of marginal zone/periosteal resorption, not readily apparent on low magnification; 2, mild, more numerous areas of marginal zone/periosteal resorption, readily apparent on low magnification, minor overall cortical and medullary bone loss; 3, moderate, obvious resorption of medullary trabecular and cortical bone without full thickness defects in entire cortex, loss of some medullary trabeculae, lesion apparent on low magnification; 4, marked, full thickness defects in cortical bone, often with distortion of profile of remaining cortical surface, marked loss of medullary bone; 5, severe, full thickness defects in cortical bone and destruction of joint architecture of all joints. For each animal, the four parameters were scored for each of the four joints analyzed and summed to obtain the individual score per parameter per mouse. Maximum score per parameter = 20/mouse. The disease sum score represents the summed scores of the individual parameters. Parameters for the various groups were then compared using a Mann-Whitney *U* test with significance set at $P \leq 0.05$. For immunohistochemistry, frozen tissue sections were fixed in cold acetone before endogenous peroxidase quenching with H_2O_2. Immunohistochemistry was performed by means of the streptavidin-biotin-peroxidase complex method using the following primary antibodies: rat anti–mouse CD8, rat anti–mouse CD4, rat anti–mouse Gr-1, hamster anti–mouse CD11c (all from eBioscience), rat anti–mouse CD68 (BioLegend). Binding of the primary antibody was revealed by specific secondary antibodies using the aminoethylcarbazole chromogenic substrate. Sections were counterstained with hematoxylin and evaluated under a DM2000 optical microscope (Leica).

In vitro stimulation of mouse blood. 5×10^5 PBMCs from huTLR8Tg chimeras or C57BL/6 WT animals were stimulated with a specific RNA-based TLR8 agonist, ORN-8L (200 μg/ml) and, 24 h later, supernatants were harvested and assayed for cytokine levels by ELISA.

In vitro assessment of TLR8 DC function. DCs were isolated using anti-CD11c magnetic beads (Miltenyi Biotec) from spleens of BM-transferred mice TLR8TgCL12>B6.SJL or C57BL/6>B6.SJL. Purity was assessed by flow cytometry and confirmed to be ∼80–90%. DC were loaded for 2 h

with 2 μg/ml $Ova_{323–339}$ washed four time and cultured with 5 × 10*4 CD4 T cells from OTII mice at the indicated concentration. Cultures were incubated for 48 h and pulsed with [^{3}H]thymidine for the last 8 h.

In vitro restimulation of T cells. Cells from spleen of TLR8TgClone 12 chimeras mice and WT mice were stimulated in vitro for 2 h with PMA (5 ng/ml) and ionomycin (500 ng/ml) in the presence of 3μγ/ml of brefeldin A. Subsequently, cells were stained for 15 min with T cells surface markers CD3, CD4, and CD8 wash and fixed and permeabilized with Cytofix/Cytoperm (BD). Fluorochrome-conjugated monoclonal antibodies to TNF, IFN-γ, IL-4, and IL-10 were used to detect intracellular cytokines (BD). Flow cytometric analyses of PBMCs and splenocytes were performed using fluorochrome-conjugated monoclonal antibodies to mouse CD3, CD4, CD8, CD44, CD62L, CD80, GITRL, OX40L, CD40, CD19, CD23, CD21, LY6G, CD11b, CD11c, F480, and FOXP3 (BD). LSRII instrument (BD) was used to acquire flow cytometer data.

Cytokines detection. Antibody pairs for measuring mouse TNF and IL-12p40 by ELISA were from RD system. TNF, IL-6, IL-17A, IL-12 p40, CCL-2 and IP-10 were determined in mouse serum by Milliplex assay (Millipore).

Real-time quantitative PCR (TaqMan) analysis. RNA was extracted from leukocytes using RNA micro kit (QIAGEN) and from pancreas tissues with fibrous tissue RNA extraction kit (QIAGEN) according to manufacturer's instructions. RNA and cDNA was generated with SuperScript First-Strand Synthesis System (Invitrogen). TAQMAN reactions were performed as described previously (Guiducci et al., 2010). Primer sequences have been previously described (Guiducci et al., 2010) and as follows: Human TLR7, forward 5′-TTACCTGGATGGAAACCAGCTACT-3′ reverse 5′-TCAAGGCTGAGAAGCTGTAAGCTA-3′, human TLR9 forward 5′-TGAAGACTTCAGGCCCAACTG-3′ reverse 5′-TGCACGGTCACCAGGTTGT-3′. Human TLR8 primer (PPH01801B-200), mouse TLR7 (PPM04208A-200), and mouse IFN-γ (PPM03121A-200) were obtained from SA Bioscience.

Patients and gene expression profiling. Pediatric patients and pediatric control were recruited at Baylor University Medical Center, Texas Scottish Rite Hospital, and Children's Medical Center, all in Dallas, TX. The Study was approved by the institutional review board of all three institutions. Informed consents were obtained from all patients (legal representatives and patients over 10 yr of age).

Blood from SoJIA pediatric patients were as follows: patients in cohort 1 (Fig. 10 A) were from day one untreated active patients in ANA-JIS clinical trial. This trial was registered at http://www.clinicaltrials.gov (registration number: NCT00339157) and details of patients are published in Quartier et al. (2011). 18 healthy age- and ethnicity-matched children were included and use to normalize the gene expression data of this cohort.

Blood samples from SoJIA pediatric patients in cohort 2 (Fig. 10 A) were from 12 patients who fulfilled the American College of Rheumatology diagnostic criteria (Cassidy et al., 1986). Patient blood was collected before starting treatment with Anakinra and after treatment (Table S1). Patients had active disease at day 1 before start of treatment and were considered in remission after Anakinra treatment. 15 healthy age- and ethnicity-matched children were included and use to normalize the gene expression data of this cohort.

Adult Systemic Onset Still's disease patients were recruited at the Baylor Rheumatology clinic in Dallas (Berry et al., 2010). Patients had systemic symptoms and/or arthritis at the time of recruitment. Still's disease patients' characteristics are summarized in Table S2. Monocytes were purified from the blood of 15 SoJIA pediatric patients with active disease Monocytes from seven healthy age- and ethnicity-matched children were included and use to normalize the gene expression data (Table S3). PBMCs were isolated by density gradient centrifugation using Ficoll-Paque PLUS (GE Healthcare). Monocytes were purified using either the EasySep Human Monocyte Enrichment kit (STEMCELL Technologies) followed by $CD14^+$ selection using MACS kits (Miltenyi Biotec).

Isolation of mouse cellular subsets. Cellular subsets were purified from spleens of B6.SJL mice transplanted with bone marrow from TLR8TgCL12 chimeras. Cellular subsets were routinely 90–95% pure. All reagents used were obtained from Miltenyi Biotec using the manufacturer's instruction. Monocytes were obtained in a two-step process. First CD11c-positive cells were depleted using magnetic beads and monocytes were purified from the negative fraction using CD11b magnetic beads. DCs were positively selected using CD11c magnetic beads. CD8 T cells were purified by first depleting CD11c- and CD11b- positive cells followed by selection of CD8-positive cells using beads. Similarly, B cells were purified after depletion of both CD11c- and CD11b-positive cells followed by positive selection of B220-positive cells. $CD4^+CD25^-$ naive T cells and $CD4^+CD25^+$ T reg were purified using their respective kit. Neutrophils were purified from the bone marrow after depletion of $CD11c^+$ cells and purification of LY6G-positive cells using magnetic beads. After purification, cells were immediately frozen in RLT buffer.

Isolation and in vitro stimulation of human cells and gene expression analysis. Whole Blood was obtained from healthy individual from Advanced Bioscience Resources. Buffy coats were obtained from the Stanford Blood Center (Palo Alto, CA). Cells were used under internal Institutional Review Board–approved protocols where all donors signed informed consent to allow the use of their blood for research purposes.

Cellular subsets were routinely 95–99% pure. mDC ($BDCA1^+$ myeloid DCs), PDC ($BDCA4^+$ plasmacytoid DCs) and naive B cells were positively selected using magnetic beads from Miltenyi Biotec. Regulatory T cells ($CD4^+CD25^+$) and $CD4^+CD25^-$ naive CD4 T cells were isolated using a T reg purification kit from Miltenyi Biotec. Untouched monocytes ($CD14^+$) were purified using a negative selection kit (Stem Cell). Untouched neutrophils were isolated using lympholyte-poly (Cedarlane Laboratories). RNA samples were extracted using the RNeasy Mini RNA Extraction kit (QIAGEN) according to manufacturer's instructions. PBMCs were stimulated as described in figure legend and RNA samples were extracted using the RNeasy Mini RNA Extraction kit (QIAGEN) according to manufacturer's instructions. Patients' blood samples for gene expression analysis were collected in Tempus tubes or ACT tube and immediately delivered to Baylor Institute for Immunology Research (Dallas, TX) at room temperature and stored at −20°C before processing.

Total RNA integrity was assessed using an Agilent 2100 Bioanalyzer showing a quality of RNA integrity number >7 (Agilent Technologies). RNA yield was assessed using a NanoDrop 1000 spectrophotometer (NanoDrop Products; Thermo Fisher Scientific). Biotinylated, amplified antisense complementary RNA (cRNA) targets were then prepared from 250 ng of the total RNA using the Illumina TotalPrep RNA Amplification kit (Applied Biosystems). 750ng of the labeled cRNA was hybridized overnight to Illumina Human HT-12 V4 BeadChip arrays (Illumina), which contained more than 47,000 probes. The arrays were then washed, blocked, stained, and scanned on an Illumina iScan following the manufacturer's protocols. Illumina GenomeStudio software v2011.1 with the Gene Expression v1.9.0 module (Illumina) was used to generate signal intensity values from the scans.

Statistical analysis. Data were analyzed using Mann Whitney Student's *t* test, unless otherwise indicated in figure legends. All analyses were performed using Prism software v5 (GraphPad Software). Differences were considered significant at $P < 0.05$.

Online supplemental material. Fig. S1 shows details of the construct used to produce the huTLRTg mice. Fig. S2 shows the pathological assessment of organs inflammation in chimera mice expressing huTLR8 generated from ES clone 12, 6, and 23. Table S1 shows SoJIA Cohort 2 patients' characteristic from Fig. 10 (A–C). Table S2 shows Still's disease patients' characteristic from Fig. 10 (A–C). Table S3 shows characteristic of the patients whose monocytes were used in experiment depicted in Fig. 10 D. Online supplemental material is available at http://www.jem.org/cgi/content/full/jem.20131044/DC1.

We would like to thank Dr. Anne O'Garra, Dr. Giorgio Trinchieri, and our colleagues at Dynavax Technologies for their critical reading of the manuscript. We are very grateful to Anthony DeFranco's laboratory members for invaluable help with performing the bone marrow transplantation experiments. We thank Gloria Esposito and Adriano Flora at TaconicArtemis GmbH for assistance on the generation of transgenic mice and Steve Noonan and Henry Lopez (Murigenics, Vallejo, CA) for assistance with animal work.

C. Guiducci, M. Gong, C. Crain, R.L. Coffman, and F.J. Barrat were full time employees of Dynavax Technologies when the study was conducted; the authors have no other conflicting financial interests.

Submitted: 20 May 2013
Accepted: 28 October 2013

REFERENCES

Ablasser, A., H. Poeck, D. Anz, M. Berger, M. Schlee, S. Kim, C. Bourquin, N. Goutagny, Z. Jiang, K.A. Fitzgerald, et al. 2009. Selection of molecular structure and delivery of RNA oligonucleotides to activate TLR7 versus TLR8 and to induce high amounts of IL-12p70 in primary human monocytes. *J. Immunol.* 182:6824–6833. http://dx.doi.org/10.4049/jimmunol.0803001

Barbalat, R., S.E. Ewald, M.L. Mouchess, and G.M. Barton. 2011. Nucleic acid recognition by the innate immune system. *Annu. Rev. Immunol.* 29:185–214. http://dx.doi.org/10.1146/annurev-immunol-031210-101340

Barrat, F.J., T. Meeker, J.H. Chan, C. Guiducci, and R.L. Coffman. 2007. Treatment of lupus-prone mice with a dual inhibitor of TLR7 and TLR9 leads to reduction of autoantibody production and amelioration of disease symptoms. *Eur. J. Immunol.* 37:3582–3586. http://dx.doi.org/10.1002/eji.200737815

Berry, M.P., C.M. Graham, F.W. McNab, Z. Xu, S.A. Bloch, T. Oni, K.A. Wilkinson, R. Banchereau, J. Skinner, R.J. Wilkinson, et al. 2010. An interferon-inducible neutrophil-driven blood transcriptional signature in human tuberculosis. *Nature*. 466:973–977. http://dx.doi.org/10.1038/nature09247

Campbell, I.K., J.A. Hamilton, and I.P. Wicks. 2000. Collagen-induced arthritis in C57BL/6 (H-2b) mice: new insights into an important disease model of rheumatoid arthritis. *Eur. J. Immunol.* 30:1568–1575. http://dx.doi.org/10.1002/1521-4141(200006)30:6<1568::AID-IMMU1568>3.0.CO;2-R

Cassidy, J.T., J.E. Levinson, J.C. Bass, J. Baum, E.J. Brewer Jr., C.W. Fink, V. Hanson, J.C. Jacobs, A.T. Masi, J.G. Schaller, et al. 1986. A study of classification criteria for a diagnosis of juvenile rheumatoid arthritis. *Arthritis Rheum.* 29:274–281. http://dx.doi.org/10.1002/art.1780290216

Christensen, S.R., J. Shupe, K. Nickerson, M. Kashgarian, R.A. Flavell, and M.J. Shlomchik. 2006. Toll-like receptor 7 and TLR9 dictate autoantibody specificity and have opposing inflammatory and regulatory roles in a murine model of lupus. *Immunity*. 25:417–428. http://dx.doi.org/10.1016/j.immuni.2006.07.013

Deane, J.A., P. Pisitkun, R.S. Barrett, L. Feigenbaum, T. Town, J.M. Ward, R.A. Flavell, and S. Bolland. 2007. Control of toll-like receptor 7 expression is essential to restrict autoimmunity and dendritic cell proliferation. *Immunity*. 27:801–810. http://dx.doi.org/10.1016/j.immuni.2007.09.009

Demaria, O., P.P. Pagni, S. Traub, A. de Gassart, N. Branzk, A.J. Murphy, D.M. Valenzuela, G.D. Yancopoulos, R.A. Flavell, and L. Alexopoulou. 2010. TLR8 deficiency leads to autoimmunity in mice. *J. Clin. Invest.* 120:3651–3662.

Döring, Y., J. Hurst, M. Lorenz, N. Prinz, N. Clemens, M.D. Drechsler, S. Bauer, J. Chapman, Y. Shoenfeld, M. Blank, et al. 2010. Human antiphospholipid antibodies induce TNFalpha in monocytes via Toll-like receptor 8. *Immunobiology*. 215:230–241. http://dx.doi.org/10.1016/j.imbio.2009.03.002

Ewald, S.E., A. Engel, J. Lee, M. Wang, M. Bogyo, and G.M. Barton. 2011. Nucleic acid recognition by Toll-like receptors is coupled to stepwise processing by cathepsins and asparagine endopeptidase. *J. Exp. Med.* 208:643–651. http://dx.doi.org/10.1084/jem.20100682

Finkelberg, D.L., D. Sahani, V. Deshpande, and W.R. Brugge. 2006. Autoimmune pancreatitis. *N. Engl. J. Med.* 355:2670–2676. http://dx.doi.org/10.1056/NEJMra061200

Forsbach, A., J.G. Nemorin, C. Montino, C. Müller, U. Samulowitz, A.P. Vicari, M. Jurk, G.K. Mutwiri, A.M. Krieg, G.B. Lipford, and J. Vollmer. 2008. Identification of RNA sequence motifs stimulating sequence-specific TLR8-dependent immune responses. *J. Immunol.* 180:3729–3738.

Fukui, R., S. Saitoh, A. Kanno, M. Onji, T. Shibata, A. Ito, M. Onji, M. Matsumoto, S. Akira, N. Yoshida, and K. Miyake. 2011. Unc93B1 restricts systemic lethal inflammation by orchestrating Toll-like receptor 7 and 9 trafficking. *Immunity*. 35:69–81. http://dx.doi.org/10.1016/j.immuni.2011.05.010

Ganguly, D., G. Chamilos, R. Lande, J. Gregorio, S. Meller, V. Facchinetti, B. Homey, F.J. Barrat, T. Zal, and M. Gilliet. 2009. Self-RNA-antimicrobial peptide complexes activate human dendritic cells through TLR7 and TLR8. *J. Exp. Med.* 206:1983–1994. http://dx.doi.org/10.1084/jem.20090480

Gantier, M.P., S. Tong, M.A. Behlke, D. Xu, S. Phipps, P.S. Foster, and B.R. Williams. 2008. TLR7 is involved in sequence-specific sensing of single-stranded RNAs in human macrophages. *J. Immunol.* 180:2117–2124.

Gorden, K.B., K.S. Gorski, S.J. Gibson, R.M. Kedl, W.C. Kieper, X. Qiu, M.A. Tomai, S.S. Alkan, and J.P. Vasilakos. 2005. Synthetic TLR agonists reveal functional differences between human TLR7 and TLR8. *J. Immunol.* 174:1259–1268.

Guiducci, C., R.L. Coffman, and F.J. Barrat. 2009. Signalling pathways leading to IFN-alpha production in human plasmacytoid dendritic cell and the possible use of agonists or antagonists of TLR7 and TLR9 in clinical indications. *J. Intern. Med.* 265:43–57. http://dx.doi.org/10.1111/j.1365-2796.2008.02050.x

Guiducci, C., C. Tripodo, M. Gong, S. Sangaletti, M.P. Colombo, R.L. Coffman, and F.J. Barrat. 2010. Autoimmune skin inflammation is dependent on plasmacytoid dendritic cell activation by nucleic acids via TLR7 and TLR9. *J. Exp. Med.* 207:2931–2942. http://dx.doi.org/10.1084/jem.20101048

Hattermann, K., S. Picard, M. Borgeat, P. Leclerc, M. Pouliot, and P. Borgeat. 2007. The Toll-like receptor 7/8-ligand resiquimod (R-848) primes human neutrophils for leukotriene B4, prostaglandin E2 and platelet-activating factor biosynthesis. *FASEB J.* 21:1575–1585. http://dx.doi.org/10.1096/fj.06-7457com

Heil, F., H. Hemmi, H. Hochrein, F. Ampenberger, C. Kirschning, S. Akira, G. Lipford, H. Wagner, and S. Bauer. 2004. Species-specific recognition of single-stranded RNA via toll-like receptor 7 and 8. *Science*. 303:1526–1529. http://dx.doi.org/10.1126/science.1093620

Hemmi, H., T. Kaisho, O. Takeuchi, S. Sato, H. Sanjo, K. Hoshino, T. Horiuchi, H. Tomizawa, K. Takeda, and S. Akira. 2002. Small anti-viral compounds activate immune cells via the TLR7 MyD88-dependent signaling pathway. *Nat. Immunol.* 3:196–200. http://dx.doi.org/10.1038/ni758

Janke, M., J. Poth, V. Wimmenauer, T. Giese, C. Coch, W. Barchet, M. Schlee, and G. Hartmann. 2009. Selective and direct activation of human neutrophils but not eosinophils by Toll-like receptor 8. *J. Allergy Clin. Immunol.* 123:1026–1033. http://dx.doi.org/10.1016/j.jaci.2009.02.015

Lan, T., E.R. Kandimalla, D. Yu, L. Bhagat, Y. Li, D. Wang, F. Zhu, J.X. Tang, M.R. Putta, Y. Cong, et al. 2007. Stabilized immune modulatory RNA compounds as agonists of Toll-like receptors 7 and 8. *Proc. Natl. Acad. Sci. USA*. 104:13750–13755. http://dx.doi.org/10.1073/pnas.0706059104

Liu, J., C. Xu, L.C. Hsu, Y. Luo, R. Xiang, and T.H. Chuang. 2010. A five-amino-acid motif in the undefined region of the TLR8 ectodomain is required for species-specific ligand recognition. *Mol. Immunol.* 47:1083–1090. http://dx.doi.org/10.1016/j.molimm.2009.11.003

Maschalidi, S., S. Hässler, F. Blanc, F.E. Sepulveda, M. Tohme, M. Chignard, P. van Endert, M. Si-Tahar, D. Descamps, and B. Manoury. 2012. Asparagine endopeptidase controls anti-influenza virus immune responses through TLR7 activation. *PLoS Pathog.* 8:e1002841. http://dx.doi.org/10.1371/journal.ppat.1002841

Mellins, E.D., C. Macaubas, and A.A. Grom. 2011. Pathogenesis of systemic juvenile idiopathic arthritis: some answers, more questions. *Nat Rev Rheumatol.* 7:416–426. http://dx.doi.org/10.1038/nrrheum.2011.68

Mouchess, M.L., N. Arpaia, G. Souza, R. Barbalat, S.E. Ewald, L. Lau, and G.M. Barton. 2011. Transmembrane mutations in Toll-like receptor 9 bypass the requirement for ectodomain proteolysis and induce

fatal inflammation. *Immunity*. 35:721–732. http://dx.doi.org/10.1016/j.immuni.2011.10.009

Nickerson, K.M., S.R. Christensen, J. Shupe, M. Kashgarian, D. Kim, K. Elkon, and M.J. Shlomchik. 2010. TLR9 regulates TLR7- and MyD88-dependent autoantibody production and disease in a murine model of lupus. *J. Immunol.* 184:1840–1848. http://dx.doi.org/10.4049/jimmunol.0902592

Pascual, V., F. Allantaz, E. Arce, M. Punaro, and J. Banchereau. 2005. Role of interleukin-1 (IL-1) in the pathogenesis of systemic onset juvenile idiopathic arthritis and clinical response to IL-1 blockade. *J. Exp. Med.* 201:1479–1486. http://dx.doi.org/10.1084/jem.20050473

Pisitkun, P., J.A. Deane, M.J. Difilippantonio, T. Tarasenko, A.B. Satterthwaite, and S. Bolland. 2006. Autoreactive B cell responses to RNA-related antigens due to TLR7 gene duplication. *Science*. 312:1669–1672. http://dx.doi.org/10.1126/science.1124978

Prinz, N., N. Clemens, D. Strand, I. Pütz, M. Lorenz, A. Daiber, P. Stein, A. Degreif, M. Radsak, H. Schild, et al. 2011. Antiphospholipid antibodies induce translocation of TLR7 and TLR8 to the endosome in human monocytes and plasmacytoid dendritic cells. *Blood*. 118:2322–2332. http://dx.doi.org/10.1182/blood-2011-01-330639

Quartier, P., F. Allantaz, R. Cimaz, P. Pillet, C. Messiaen, C. Bardin, X. Bossuyt, A. Boutten, J. Bienvenu, A. Duquesne, et al. 2011. A multicentre, randomised, double-blind, placebo-controlled trial with the interleukin-1 receptor antagonist anakinra in patients with systemic-onset juvenile idiopathic arthritis (ANAJIS trial). *Ann. Rheum. Dis.* 70:747–754. http://dx.doi.org/10.1136/ard.2010.134254

Sacre, S.M., A. Lo, B. Gregory, R.E. Simmonds, L. Williams, M. Feldmann, F.M. Brennan, and B.M. Foxwell. 2008. Inhibitors of TLR8 reduce TNF production from human rheumatoid synovial membrane cultures. *J. Immunol.* 181:8002–8009.

Sarvestani, S.T., B.R. Williams, and M.P. Gantier. 2012. Human Toll-like receptor 8 can be cool too: implications for foreign RNA sensing. *J. Interferon Cytokine Res.* 32:350–361. http://dx.doi.org/10.1089/jir.2012.0014

Sparwasser, T., and G. Eberl. 2007. BAC to immunology—bacterial artificial chromosome-mediated transgenesis for targeting of immune cells. *Immunology*. 121:308–313. http://dx.doi.org/10.1111/j.1365-2567.2007.02605.x

Subramanian, S., K. Tus, Q.Z. Li, A. Wang, X.H. Tian, J. Zhou, C. Liang, G. Bartov, L.D. McDaniel, X.J. Zhou, et al. 2006. A Tlr7 translocation accelerates systemic autoimmunity in murine lupus. *Proc. Natl. Acad. Sci. USA*. 103:9970–9975. http://dx.doi.org/10.1073/pnas.0603912103

Vollmer, J., S. Tluk, C. Schmitz, S. Hamm, M. Jurk, A. Forsbach, S. Akira, K.M. Kelly, W.H. Reeves, S. Bauer, and A.M. Krieg. 2005. Immune stimulation mediated by autoantigen binding sites within small nuclear RNAs involves Toll-like receptors 7 and 8. *J. Exp. Med.* 202:1575–1585. http://dx.doi.org/10.1084/jem.20051696

Walsh, E.R., P. Pisitkun, E. Voynova, J.A. Deane, B.L. Scott, R.R. Caspi, and S. Bolland. 2012. Dual signaling by innate and adaptive immune receptors is required for TLR7-induced B-cell-mediated autoimmunity. *Proc. Natl. Acad. Sci. USA*. 109:16276–16281. http://dx.doi.org/10.1073/pnas.1209372109

Wang, J., Y. Shao, T.A. Bennett, R.A. Shankar, P.D. Wightman, and L.G. Reddy. 2006. The functional effects of physical interactions among Toll-like receptors 7, 8, and 9. *J. Biol. Chem.* 281:37427–37434. http://dx.doi.org/10.1074/jbc.M605311200

Zandieh, I., and M.F. Byrne. 2007. Autoimmune pancreatitis: a review. *World J. Gastroenterol.* 13:6327–6332. http://dx.doi.org/10.3748/wjg.13.6327

SUPPLEMENTAL MATERIAL

Guiducci et al., http://www.jem.org/cgi/content/full/jem.20131044/DC1

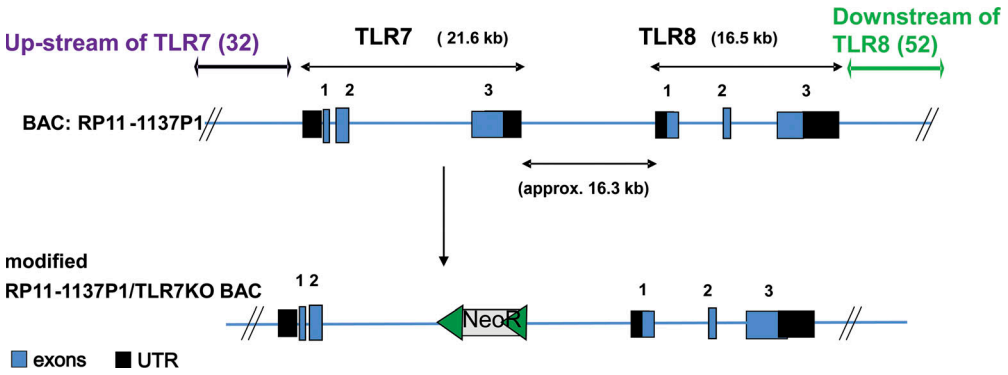

Figure S1. Details of the construct used to produce the huTLRTg mice. The TLR8 BAC construct used to produce the TLR8 transgenic mice. Transgenic TLR8 mice were generated using BAC/ES technologies (Sparwasser and Eberl, 2007) at Taconic. In brief, the human BAC carrying TLR8 gene was obtained from the RPCIB-753 BAC library. The human BAC contains both human TLR7 and TLR8 genes in a cluster. The BAC was modified to knock out TLR7 gene and to retain the chromosomal region at the 5′UTR of mouse TLR8 that contains the promoter. To inactivate the TLR7 gene on the RP11-1137P1 BAC, TLR7 exon 3 encoding most of the protein was replaced with an FRT-flanked Neomycin Resistance (NeoR) cassette. The modified BAC construct, BAC_RP11-1137P1_TLR7-KO was transfected into an ES cell line, C57BL/6NTac ES cell line using Lipofectamine (Invitrogen) according to manufacturer's protocol. From day 2 onwards the medium was replaced daily with medium containing 200 µg/ml G418 (Geneticin; Invitrogen). 7 d later, single clones were isolated, expanded, and analyzed by Southern blot for detection of genomic insertion. Four clones were chosen with a range of inserted human TLR8 in the genome. Clone 8 and 6 contains ∼1-2 copies of the gene; clone 12 contains 2–4 copies and clone 23 contains ∼15 copies. Those ES clones were injected into the blastocoel of 3.5-d-old mouse blastocysts from BALB/c females. Subsequently, the injected embryos were transferred to the uterine horns of appropriately timed pseudopregnant recipient BALB/c females. Embryos gestated for ∼18 d, and the resulting pups were chimeras, whose tissues have developed from both the ES cells carrying TLR8 gene (C57BL/6 background) and the recipient blastocyst cells of BALB/c background. This mix of starter cells was visible in the mouse's coat, which exhibited patches of coat color from the host embryo and patches from the injected ES clone. Chimeras with 25–75% ES contribution (based on fur color) were then put to breed with C57BL/6 animals to pass germline transmission. Chimeras generated using ES clone 8 were the only one that passed germline. The other failed to breed and showed rapid sign of disease.

A

TLR8 Clones	Mice	Pancreatitis	Kidney GN	Kidney Pyelitis	Liver Cholangitis
TLR8TgCL12	1	2.5	1.5	0.0	1.0
	2	2.5	2.5	0.0	2.5
	3	4.0	0.5	0.5	1.5
	4	4.0	1.0	0.5	2.5
	5	3.5	2.5	2.5	2.5
	6	3.0	2.0	1.0	2.5
	7	4.0	2.5	2.5	2.0
	8	4.0	2.0	2.0	2.5
	9	3.5	2.5	/	2.5
	10	4.0	2.5	3.0	3.5
	11	/	2.5	1.0	2.0
	12	/	2.5	1.0	2.5
	13	/	2.5	2.0	2.0
	14	/	2.5	2.5	3.0
	15	/	2.5	3.0	3.5
	16	/	2.5	2.0	4.0
	17	/	3.0	1.0	3.0
	18	/	2.5	2.0	3.5
TLR8TgCL23	1	3.5	3	2.5	2
	2	3.5	/	/	3
	3	4.0	3	2.0	4
	4	4.0	3	0.0	2
TLR8TgCL6	1	4.0	2.5	2.5	0.0
	2	4.0	2.5	2.0	1.0
	3	4.0	2.5	2.5	2.0
	4	4.0	2.5	3.0	3.5
	5	4.0	2.5	3.0	3.0
	6	4.0	2.5	2.5	1.0
Total TLR8 Tg mice (N=28)	**AVERAGE**	**3.7**	**2.3**	**1.8**	**2.4**
	SEM	*0.1*	*0.1*	*0.2*	*0.2*
Ctrl mice (N=14)	**AVERAGE**	**0.0**	**1.1**	**0.6**	**0.2**
	SEM	*0.0*	*0.2*	*0.2*	*0.1*
Stats	P values	< 0.0001	0.001	0.01	< 0.0001

Chimeras were sacrificed when moribund. Age of mice ranged from 44-140 days for Clone 12; 23-50 days for Clone 6; 28-64 days for Clone 23. 14 mice C57BL/6 age 50-150 days old were used as CTRL. Histological features was scored singularly and graded 1 to 4 as Specified in Materials and Methods. p values are in between transgenic mice and control mice. GN: (Glomerulonephritis).

B

	Pancreas		Kidney		Liver	
	WT	TLR8Tg	WT	TLR8Tg	WT	TLR8Tg
CD8+ T cells	3±0.3	10±0.5[a]	4±0.2	9±1[a]	5±0.3	9±1[a]
CD4+ T cells	5±1	9±1[b]	5±1	6±1	4±1	8±1[b]
(CD11c$^+$) DC	2±0.4	6±0.4[a]	2±0.3	6±0.5[a]	3±1	6±1[b]
CD68$^+$(macrophages)	2±1	10±1[a]	3±0.4	9±1[a]	nd	nd
GR1$^+$ (neutrophils)	4±1	10±1[a]	4±1	6±1	4±1	10±1[a]

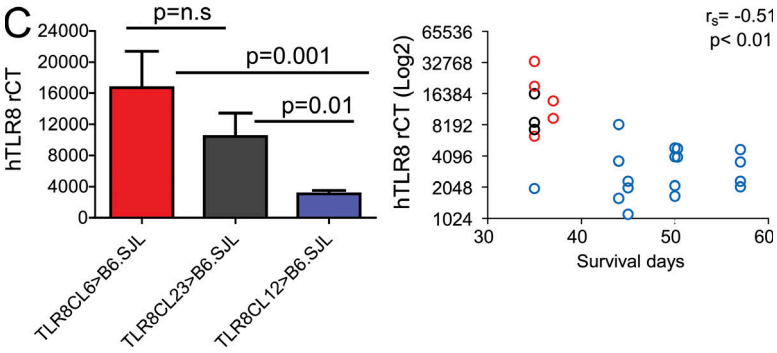

Figure S2. Pathological assessment of organs inflammation in chimera mice expressing huTLR8 generated from ES clone 12, 6, and 23. (A) Chimera mice were sacrificed when moribund. Age of mice ranged from 44–140 d for TLR8 TgCL12 chimera mice; 23–50 d for TLR8TgCL6 chimera mice; 28–64 d for LR8TgCL23 chimera mice. 14 mice C57BL/6 age 50–150-d-old were used as CTRL. Histological features were scored singularly and graded 1–4 as indicated in the method section. Kidney lesions consisted of pyelitis and glomerulonephritis. Pyelitis consisted of increased numbers of lymphocytes and macrophages within the connective tissue adjacent to the epithelium that lines both the calyxes and papilla, with increased fibrous connective tissue. Glomerulonephritis was characterized by combinations of the following: enlargement of the glomerulus with loss of structure, segmental to diffuse hypercellularity owing to mesangial proliferation and focal collections of lymphocytes within the cortical interstitium, sometimes with focal fibroplasia. Liver inflammatory reaction was characterized by accumulation of the inflammatory reaction in the portal area with increased fibrous connective tissue that contained numerous lymphocytes and macrophages. Similarly affected were salivary glands that were severely compromise by a similar inflammatory infiltrate to what seen in the other organs (not depicted). (B) Immunohistochemistry analysis of organs from TLR8TgCL12 chimera mice. Mice were sacrificed when moribund and organs were collected and included in OCT medium. Analysis of the inflammatory infiltrate in the pancreas, kidney, and liver confirmed the prominent participation of CD68$^+$ macrophages, T cells, CD11c$^+$ DCs, and Gr-1$^+$ neutrophils to the composition of the infiltrates. In contrast, no significant infiltration of B cells was detected at the same time point. The number of immunoreactive cells was counted out of five 400× magnification high-power microscopic fields by a blinded pathologist. Mean ± SEM number of mice evaluated (6 per group). A = $P < 0.001$; b = $P < 0.01$. (C) huTLR8 expression level in B6.SJL- mice mice transplanted with bone marrow from huTLR8Tg chimeras correlate with survival. Gene expression was evaluated in spleens of BM-transplanted animals; $n = 18$ for TLR8TgCL12>B6.SJL (blue); $n = 5$ for TLR8TgCL6>B6.SJL (red); $n = 3$ for TLR8TgCL23>B6.SJL (black).